Received: 2 February 2022 | Revised: 2 August 2022 | Accepted: 9 August 2022

DOI: 10.1111/bre.12711

Basin Research | IAS EAGE | WILEY

RESEARCH ARTICLE

Provenance of Oligocene lithic and quartz arenites of the East Carpathians: Understanding sediment routing systems on compressional basin margins

Relu D. Roban[1,2] | **Mihai N. Ducea**[1,3] | **Vlad I. Mihalcea**[1] | **Ioan Munteanu**[1] | **Victor Barbu**[4] | **Mihaela C. Melinte-Dobrinescu**[1,2] | **Cornel Olariu**[2,5] | **Mihai Vlăsceanu**[1]

[1]Faculty of Geology and Geophysics, University of Bucharest, Bucharest, Romania

[2]National Institute of Marine Geology and Geo-Ecology, Bucharest, Romania

[3]Department of Geosciences, University of Arizona, Tucson, Arizona, USA

[4]OMV Petrom, Bucharest, Romania

[5]Jackson School of Geosciences, University of Texas at Austin, Austin, Texas, USA

Correspondence
Relu D. Roban and Ioan Munteanu, Faculty of Geology and Geophysics, University of Bucharest, Bucharest, Romania.
Email: reludumitru.roban@g.unibuc.ro and ioan.munteanu@unibuc.ro

Funding information
Romanian Executive Agency for Higher Education, Research, Development and Innovation, Grant/Award Number: PN-III-P4-PCE-2021-0901, PN-III-P4-PCE-2020-0971 and PN-III-P4-ID-PCCF-2016-0014

Abstract

We present new sedimentological, petrographical, palaeontological and detrital zircon U–Pb data on late Oligocene–early Miocene sedimentary rocks of the thin-skinned thrust belt of East Carpathians. These data were acquired to reconstruct the sedimentary routing system for two compositionally different turbidite fans made of the regionally extensive Kliwa and Fusaru formations. On the eastern margin of the Moldavides foreland basin, large low-gradient river systems draining the East European Platform provided well-sorted quartz-rich sand forming deltas on wide shallow shelves and thick Kliwa submarine fans. Due to the westward subduction of a thinned continental plate, the western basin margin was characterized by short, steep-gradient routing systems where sediment transport to deep water was mainly through hyperpycnal flows. The Getic and Bucovinian nappes of the East Carpathians and the exhumed Cretaceous–Early Palaeogene orogenic wedge fed Fusaru fans with poorly sorted lithic sand. The Fusaru fans trend northwards in the foredeep basin having an elongate depocentre, interfingering and then overlapping on the distal part of the Kliwa depositional system due to the eastward advance of the Carpathian fold-and-thrust belt. A smaller sediment input is supplied by southern continental areas (i.e. Moesian Platform, North Dobrogea and potentially the Balkans). In general, the sandstone interfingering between distinct basin floor fan systems is less well documented because the facies would be similar and there are not many systems that have a distinct sediment provenance like Kliwa and Fusaru systems. This case study improves the understanding of regional palaeogeography and sedimentary routing systems and provides observations relevant here or elsewhere on the interfingering turbidite fan systems.

KEYWORDS

detrital zircons, East Carpathians, foreland basin, Oligocene, sandstone provenance, turbidites

© 2022 International Association of Sedimentologists and European Association of Geoscientists and Engineers and John Wiley & Sons Ltd.

1 | INTRODUCTION

Many clastic sedimentary systems contain four main segments from source to sink: river catchment area; continental shelf; continental slope and submarine fan (Allen, 2017; Nyberg et al., 2018; Sømme et al., 2009). The deposits preserved within orogenic belts rarely display the complete sedimentary record of typical source-to-sink systems because of erosion or burial of one or several segments. Ancient sediment routing systems are usually reconstructed by the means of petrography and heavy minerals analysis coupled with facies modelling. Using the extent of modern routing systems that are controlled by similar tectonic and climatic regimes as analogs offer additional constraints.

The Romanian Carpathians (Figure 1a) represents a collage of tectonic units (Tisza, Piennides, East-Vardar, Dacia, Ceahlău-Severin and Moesia-Danubian, Figure 1b,c) that were gradually assembled during the closure of East Vardar and Ceahlău-Severin oceanic basins that can be linked to the evolution of the Neotethys and Alpine Tethys. The Oligocene deposits of the external thin-skinned nappes of the East Carpathians, namely the Moldavides (Săndulescu, 1984) comprise mainly deep-water facies (submarine fan and pelagic basin floor), thus the link to their source areas is poorly understood. Floored by a thinned continental crust, the Moldavides Basin represents the eastern part of the Ceahlău-Severin Ocean, which opened in the Middle Jurassic (Schmid et al., 2008). The Ceahlău sector was progressively shortened after the onset of subduction in the latest Early Cretaceous and during an episode of Palaeogene–Pliocene continental collision, involving the downgoing European plate and the overriding Dacia mega-unit (Mațenco, 2017; Săndulescu, 1984; Schmid et al., 2008, 2020; Van Hinsbergen et al., 2020). After isolation from the Mediterranean Sea in the Early Oligocene (Rögl, 1999; Rusu, 1988), the Moldavides foreland basin became part of the Central Paratethyan Domain, and developed anoxic conditions depositing organic-rich shales with TOC >2% (Sachsenhofer et al., 2015, 2018). These bituminous shales form hydrocarbon source rocks, and their deposition continues up to the Early Miocene (Dicea, 1996; Popescu, 1995; Săndulescu, 1988). Oligocene anoxia conditions alternated with gravity-driven sedimentation in the form of mass-transport deposits and sandy turbidites sourced from opposite margins of the foreland basin (Anastasiu et al., 1994; Miclăuș et al., 2009; Schieber et al., 2019). Several publications focused on the Polish Outer Carpathians described shallow-water facies co-eval to deep water deposits and interpreted on the basis of storm-generated structures and palaeontological data (e.g. Dziadzio et al., 2016). Previous works (i.e. Grasu et al., 1988; Vinogradov et al., 1983) showed that the texturally mature, quartz-rich sandstone of the Kliwa Formation was sourced from the eastern margin, while the poorly sorted lithic clastic material of the Fusaru Formation was fed from the Carpathian Orogen on the western margin. Numerous studies on the East Carpathians' Oligocene deposits focused on hydrocarbon exploration and production. However, up-to-date sedimentological, petrographical, biostratigraphical and geochronological studies are needed to better describe the origin as well as the spatial and temporal relationship between Fusaru and Kliwa formations, the main Oligocene turbidite units of the East Carpathians.

This work aims to answer the following questions: (i) Were the Kliwa and Fusaru formations deposited simultaneously? (ii) Which were the controllers for the low textural maturity of the Fusaru Formation, and the high textural maturity, of the quartzous composition of the Kliwa Formation? (iii) What were the potential sediment source areas and routing systems that lead to the deposition of these shallow to deep source-to-sink sedimentary systems? (iv) Was the sedimentation controlled by climate or tectonics? To answer these questions, we acquired and interpreted new sedimentological, petrographical, biostratigraphical and zircon DZ geochronological data that allowed us to construct a clearer image of the Oligocene source-to-sink system and its deep-water component preserved in the East Carpathians.

Highlights

- Sources of Oligocene arenites deposited in the foreland basin were identified and their routing systems were reconstructed.
- Quartz-rich sandy turbidites were supplied through long systems from eastern foreland units.
- Lithic sandy turbidites were connected by short drainage systems with the western exhumed orogen.
- The mixture of sands recorded is a consequence of source areas activation and reworking by basin currents.

2 | GEOLOGICAL SETTING

2.1 | Tectonics and stratigraphy of the East Carpathian fold and thrust belt

Following the Middle Jurassic–Early Cretaceous opening and enlargement of the Ceahlău-Severin Ocean, the latest Early Cretaceous–Eocene tectonic compressional

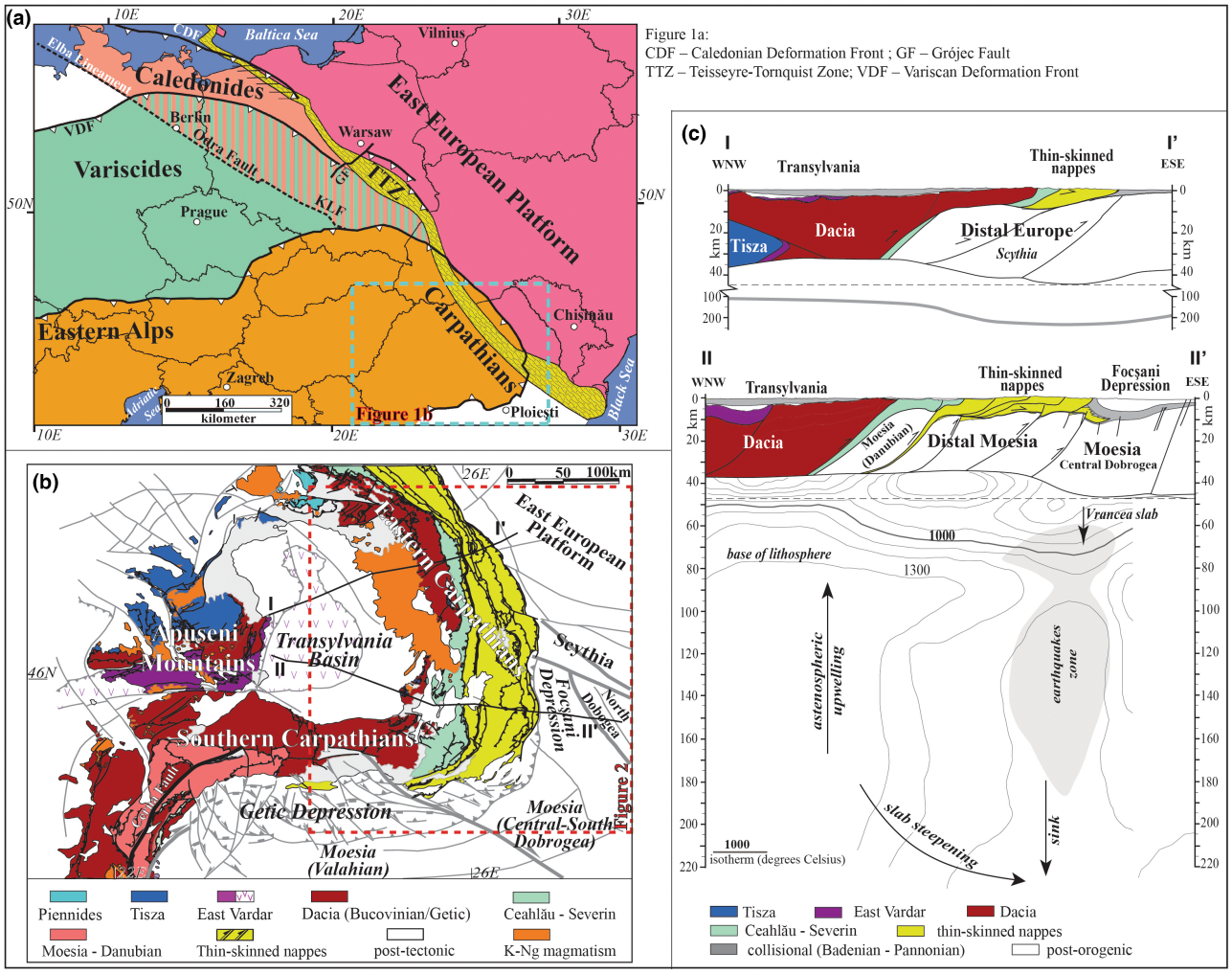

Figure 1a:
CDF – Caledonian Deformation Front ; GF – Grójec Fault
TTZ – Teisseyre-Tornquist Zone; VDF – Variscan Deformation Front

FIGURE 1 (a) The location of the Carpathians in the European Alpine belt and the relationship with the Teisseyre–Tornquist Zone (TTZ) and the edge of the East-European Platform (after Mazur et al., 2018). The inset is the location of b; (b) The simplified tectonic map of the Romanian Carpathians (after the Geological Institute of Romania—GIR maps; Mațenco, 2017 and references therein). The location of cross sections I–I′ and II–II′ are shown in c. The inset is the location of Figure 2; (c) W-E cross sections across the Transylvanian Basin, East and South Carpathians and their foreland, slightly modified from (Mațenco, 2017; Tiliță et al., 2018).

inversion led to the formation of thick-skinned nappes (Getic/Bucovinian nappes, part of Dacia mega-unit; Figure 1b,c) and to the Severin and Ceahlău nappe complex, an oceanic suture accreted to the Dacia mega-unit (Săndulescu, 1984; Schmid et al., 2020; Ștefănescu, 1976). The Ceahlău nappe complex of the East Carpathians (Figure 2) contains only upper Middle Jurassic–Cretaceous sediments and some mafic magmatic rock fragments interpreted as ophiolites (Săndulescu, 1984, 1988). A major event is recorded during the late Eocene when large scale uplift took place in the external orogenic wedge (Figure 3a), as an effect of the continental collision between the Tizsa-Dacia block and the thinned continental European plate (including distal Moesia/Danubian), after the Ceahlău Ocean consumption (Necea et al., 2021 and references therein), resulting in the formation of the Moldavides foreland basin (sensu DeCelles & Giles, 1996). The forelandward deformation, trench migration and exhumation process continued during the Oligocene–Pliocene interval (Mațenco & Bertotti, 2000; Răbăgia et al., 2011).

The Moldavides Nappes (Săndulescu, 1984) comprise the Inner Moldavides (Teleajen, Macla and Audia nappes) and the Outer Moldavides (Tarcău, Vrancea and Subcarpathian nappes), (Figures 2 and 3b). The inner Moldavide units contain deep-water sediments of Lower Cretaceous (Valanginian)–Eocene age (Roban et al., 2017, 2020; Ștefănescu et al., 2006). The incorporation of the inner Moldavide thin-skinned Teleajen, Macla and Audia nappes took place in the late Oligocene–early Miocene (Figure 3a–c), based on unconformities and geometric relationships with post-tectonic deposits (Răbăgia et al., 2011; Ștefănescu et al., 2006). The deformation of these units was coeval with the initiation of the rapid Vrancea slab

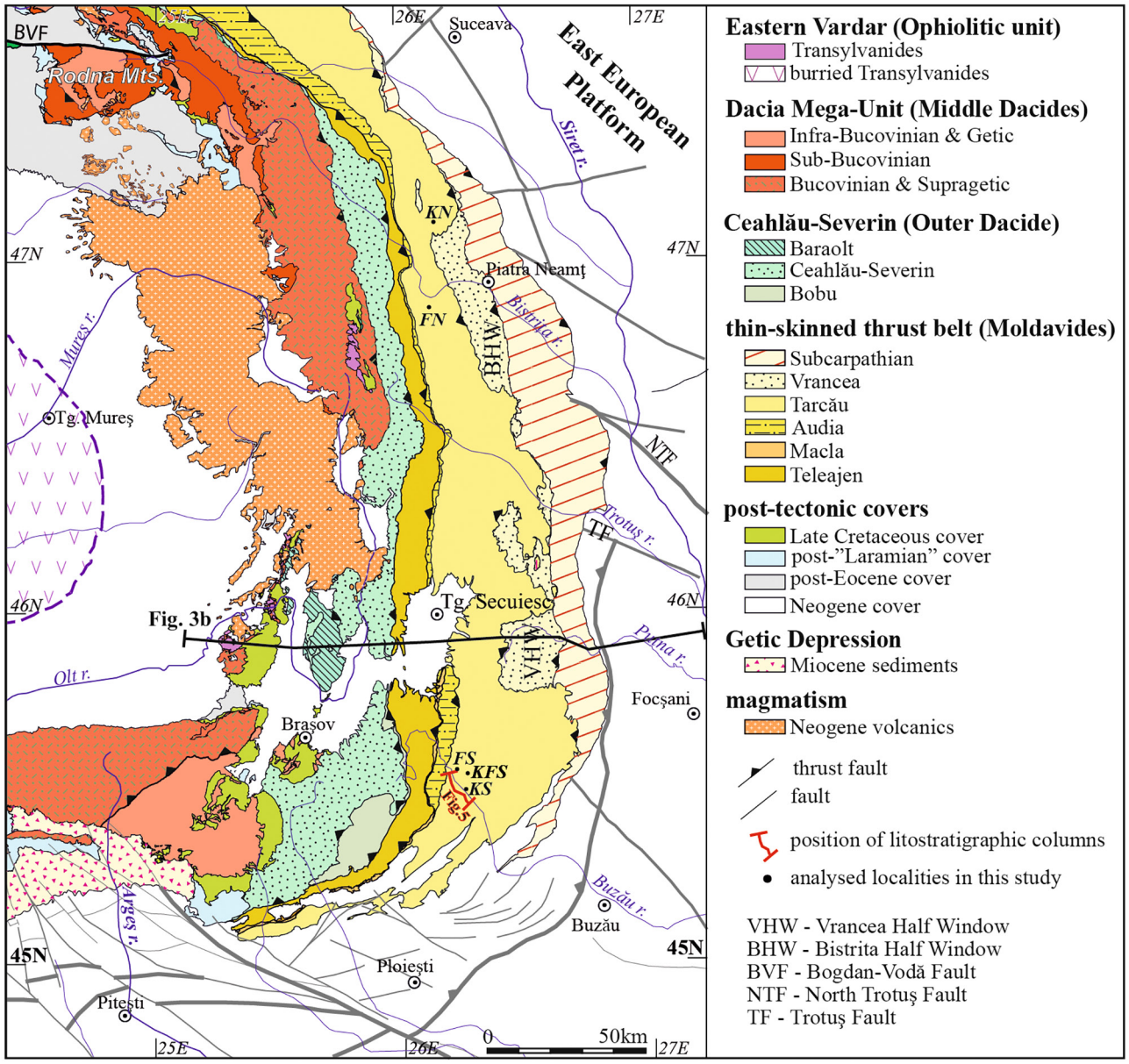

FIGURE 2 A detailed fragment of the tectonic map displayed in Figure 1b, focusing on the East Carpathians, after Geological Institute of Romania maps, Mațenco (2017) and references therein. The black line shows the location of the geological section from Figure 3b. The red line indicates the sections from Figure 5: FN (Fusaru North—Tarcău locality); KN (Kliwa North—Sihla locality); FS (Fusaru South—Siriu Dam Lake), KS (Kliwa South—Buzău Valley, Șețu rail station) and KFS (Kliwa and Fusau South—Vinețișu locality) are the locations of the sections described in this study.

roll-back (Figure 1c) and trench retreat accompanied by shortening in the Moldavides Basin and back-arc extension in the Pannonian Basin at around 20 Ma (Horváth et al., 2015). The shortening continued during the Middle Miocene and formed the Tarcău and Vrancea nappes (Mațenco & Bertotti, 2000; Săndulescu, 1988). These are mostly composed of deep-water Lower Cretaceous to lower Miocene deposits (Ștefănescu et al., 2006). The largest proportion of Oligocene deposits is found within the Tarcău Nappe, which was analysed in this work (Figure 4). The ages of the Oligocene sediments were assigned based on calcareous nannofossil biostratigraphy because other macro-and micro-fossils are mostly lacking (Figure 5). The Eocene–Oligocene boundary (Figure 4) is situated above the Globigerina Marls level, coincident with the occurrence of the 'Bituminous Marl' Formation (NP21 biozone) (Melinte, 2005; Ştefănescu et al., 1979). The Rupelian–early Chattian (NP22—base of NP24) is composed of organic-rich hemipelagic deposits (shales-dysodiles and dark cherts-menilites), while sandy turbidites (Fusaru and Kliwa formations) were deposited during the upper Oligocene (Chattian, NP24-NN1 biozone,

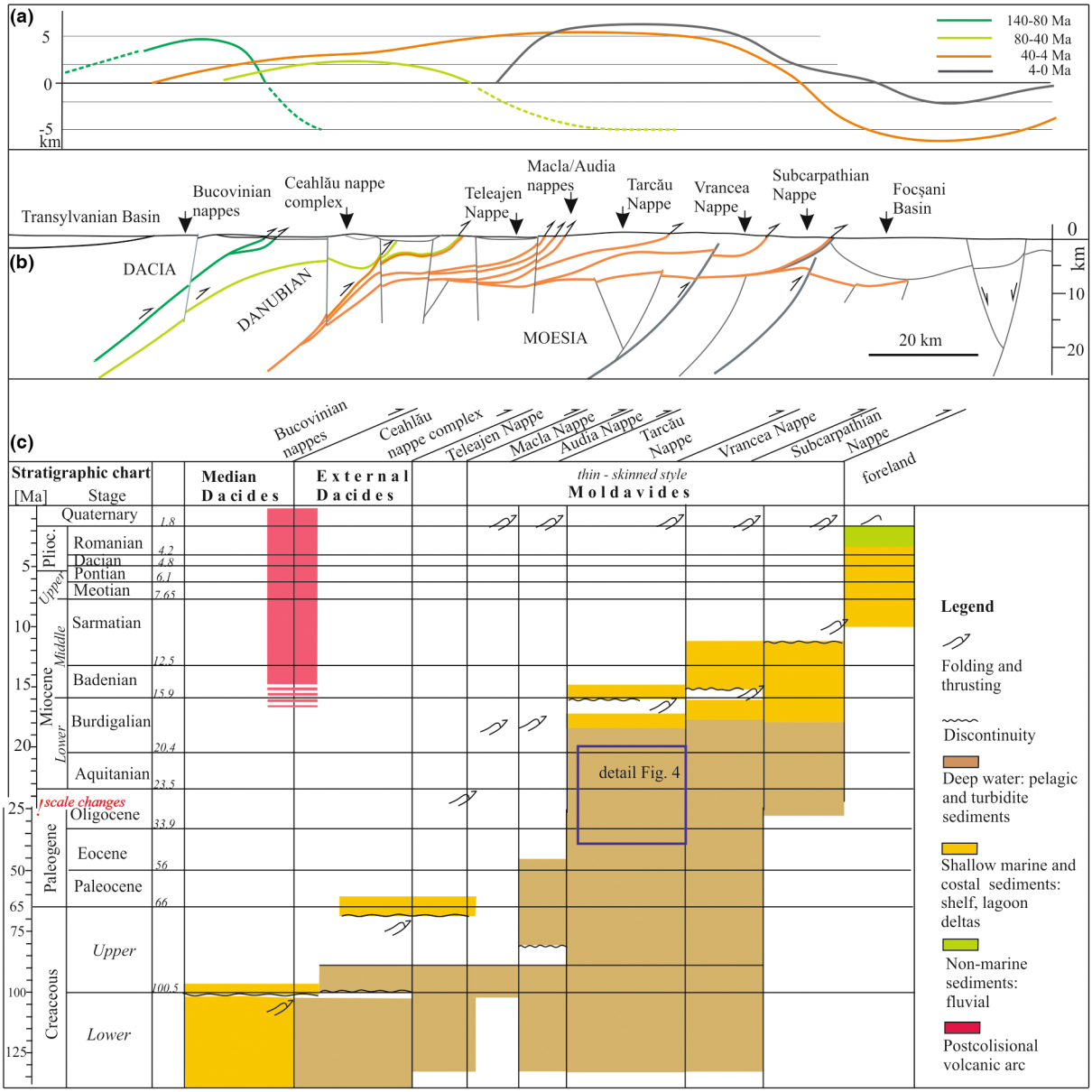

FIGURE 3 (a) The exhumation/burial time peak intervals of the East Carpathian tectonic units based on high-resolution low-temperature (apatite fission-track and U-Th/He) thermochronologic data (after Necea et al., 2021). During the Cretaceous–Quaternary interval, the exhumation advanced to the east; (b) Geological cross section through the East Carpathians after (Merten et al., 2010). The thrust faults bounding the nappes are coloured according to their timing, which correlates with the exhumation intervals displayed in a; (c) Simplified tectono-stratigraphical chart of the East Carpathians illustrating the depositional and structural relationships of the east-vergent nappes, and depositional environments, modified after Săndulescu, Kräutner, et al. (1981); Săndulescu, Ștefănescu, et al. (1981); 1:50,000 and 1:200,000 geological maps published by the Geological Institute of Romania, and Merten et al. (2010); Mațenco (2017); Roban et al. (2020). Post-tectonic sedimentation overlying nappes are not displayed.

Figure 5). The Vrancea Nappe, located eastward of the Tarcău Nappe (Figure 2), has roughly the same Oligocene stratigraphy (Figure 4), with the addition of a conglomeratic unit (Piatra Geamană Formation) dominated by low-grade metamorphic green clasts which might indicate a source area located at the edge of the East European Platform (Roban et al., 2020). The incorporation of the Subcarpathian Nappe (Figures 2 and 3c) into the orogenic system took place during middle-late Miocene times (12 to 8 Ma), with deformation being gradually transferred backward into the internal fold-and-thrust belt units (Ștefănescu et al., 2006). This nappe contains a thick turbiditic succession that transitions laterally into shallow-water deposits of the Eocene to late Miocene age. The calculated minimum amount of shortening of the East Carpathian fold-and-thrust belt in the Miocene increases northward from 140 to 160 km in the East Carpathian Bend Zone to 220–240 km in the Polish Carpathians

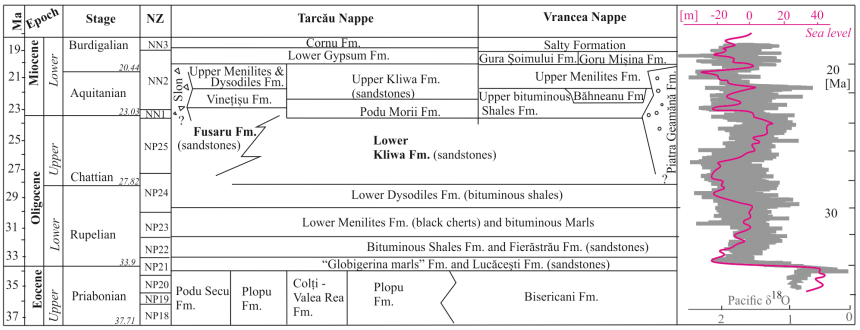

FIGURE 4 Eocene–lower Miocene stratigraphy of the Tarcău and Vrancea nappes, modified after Săndulescu, Ștefănescu, et al. (1981); Ștefănescu et al. (2006). Ages of nannofossil zones (NZ) after Gradstein et al. (2004). Ages of the lithostratigraphical formations (Fm.) after Melinte (2005). On the right side, is the summary of Oligocene benthic foraminiferal $\delta^{18}O$, and global sea-level records (after Miller et al., 2020).

(Ellouz & Roca, 1994; Gągała et al., 2012; Morely, 1996; Roure et al., 1993). The 15 to 11 Ma exhumation event (Necea et al., 2021) recorded in all the external nappes is related to limited out-of-sequence deformation affecting the internal nappes. The post 8 Ma exhumation event is associated with the emplacement of the Subcarpathian Nappe and locking of the Pericarpathian leading thrust (Mațenco et al., 2010). The later event was recorded mostly in the external nappes and in the western flank of the Focșani foredeep basin, which contains a large proportion of Miocene-Quaternary sediments with thicknesses greater than 13 km (Tărăpoancă et al., 2003) deposited in shallow water, deltaic and continental environments (Andreescu et al., 2013). The 5 km Plio-Quaternary shortening recorded in the western flank of the Focșani Basin (Hippolyte et al., 1996; Leever, Bertotti, et al., 2006; Leever, Mațenco, et al., 2006) is coeval with the small-scale extension recorded in the internal part of the East Carpathian Bend Zone, as proven by the presence of the Brașov–Târgu Secuiesc intra-mountainous basins (Figure 2). The reactivation of pre-existing deep, high-angle faults (Mațenco et al., 2010) and slab pull are processes considered responsible for the rapid, asymmetric, deeper to the west subsidence of the Focșani Basin, involving the eastward migration of the depocentre and differential uplift recorded by thin-skinned nappes (Necea et al., 2021). The Miocene (~15 Ma) to the Quaternary volcanic arc is located at the western margin of the East Carpathians (Figure 2) and is composed of andesites with some basalts and rhyolites (Seghedi et al., 2011). The volcanic chain is related to the subduction and subsequent rupture of the Vrancea Slab (i.e. Ducea et al., 2020; Seghedi et al., 2011). Apatite (U-Th)/He and fission-track data (Merten et al., 2010; Necea et al., 2021) suggest that at least the Bucovinian and Ceahlău complex nappes have been uplifted during Oligocene, providing the source for the internal part of the Moldavides Basin deposits (Figure 3a,b).

2.2 | Review of the zircon U–Pb geochronology of the main source areas around to Moldavides Basin

The Oligocene Moldavides foreland basin-fill sediments are most likely sourced from the adjacent continental areas, the thick-skinned thrust sheets of the Dacia mega-unit together with the Ceahlău-Severin Suture (Figure 3b) which was already exhumed during the Oligocene (Necea et al., 2021). Underlying the post-Carboniferous sedimentary cover of the Dacia mega-unit is a basement composed of Neo-proterozoic to Silurian islands arc terranes. Some of them underwent metamorphism immediately after their formation (Ordovician to Silurian), whereas others were metamorphosed during the Variscan Orogeny, between 350 and 320 Ma (Ducea et al., 2016; Medaris et al., 2003). Ordovician age peaks (Balintoni & Balica, 2013; Balintoni, Balica, Ducea, et al., 2010) mark a significant magmatic flux at around 465 Ma (Stoica et al., 2016). Other important peaks are present at 520, 540, 580 and 600 Ma (Balintoni et al., 2014). However, the overall amplitude of the density curve decreases towards 750 Ma, typical of peri-Gondwana terranes of central and East Europe and metamorphics of Anatolia, Iran and the Caucasus (Stern, 1994). A less pronounced peak at 325–340 Ma can be correlated with the Variscan orogeny, coinciding with a period of regional metamorphism (Ducea et al., 2018) although most zircons of that age are magmatic (Figure 6a,b). The Albian deposits covering the front of the Getic Nappe (Bucegi Conglomerates; Săndulescu, 1984) and the ones within the Teleajen-Audia nappes (Figure 6a,b) show similar age distribution profiles and U/Th pattern to those of the Dacia mega-unit (Roban et al., 2020, 2022; Stoica et al., 2016).

Bounding the Oligocene Moldavides Basin to the south and east, the European realm represents a collage of tectonic units (Figure 1b) assembled at the end of the Palaeozoic comprising a Precambrian to Palaeozoic

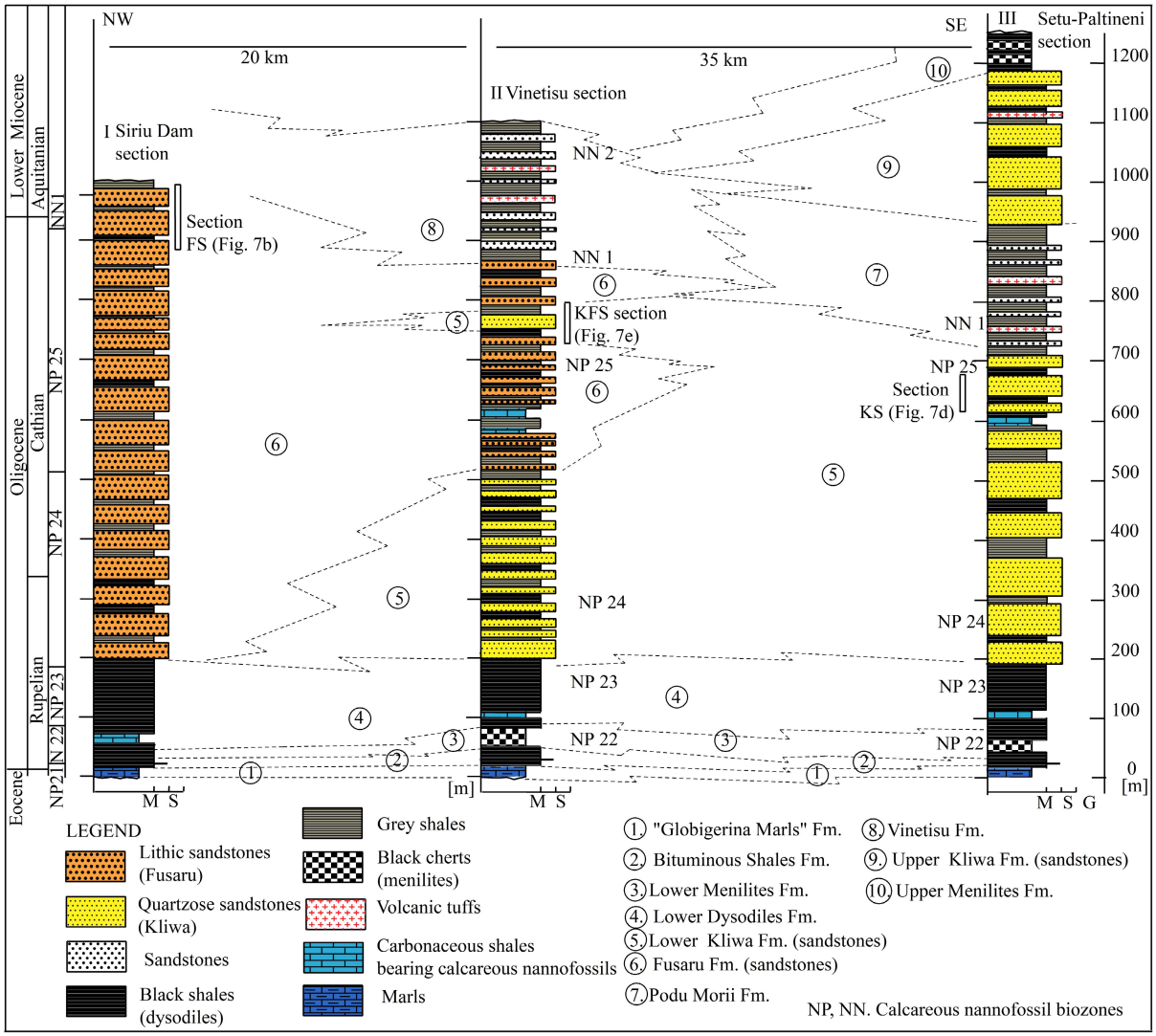

FIGURE 5 Lithostratigraphical logs of the southern profile across the East Carpathians along the Buzău River. The location of the sections is marked in Figure 2. Note the Fusaru and Kliwa formations interfingering zone (central-southern section, Vinețișu Valley left tributary of the Buzău Valley) was redrawn after (Ștefănescu et al., 1993). Calcareous nanoplankton (NP) biozones after Melinte (2005); Ștefănescu et al. (2018) and this paper.

basement overlain by sedimentary deposits: (i) the East European Platform, which has a Precambrian basement and a Neo-proterozoic to Quaternary sedimentary cover; (ii) the Scythian Platform, considered to be the SE margin of the East European Platform, which was affected by repeated deformation cycles during the Proterozoic–Peleozoic interval (Saintot et al., 2006); (iii) the Moesian Platform, which has an Proterozoic-Cambrian basement (Balintoni, Balica, Ducea, et al., 2011; Oaie et al., 2005) outcropping in Central Dobrogea (part of Moesia) and a their sedimentary cover; (iv) North Dobrogea, located between the Scythian Platform and Central Dobrogea thought as a part of the Cimmerian Orogen, containing high-angle thrust sheets which also include elements of the Variscan Orogen (Seghedi, 2001); (v) the Danubian Unit, part of the European margin (Moesia), which were deformed mainly during the Cretaceous and subsequently exhumated in the Eocene, as a result of the Dacia-Moesia continental collision (Mațenco & Schmid, 1999; Seghedi et al., 2005). Caution is needed when referring to these units, including the western margin of the East European Craton, as legitimate platform areas since they were subjected to deformation and/or magmatic activity throughout most of Earth's history (Ducea et al., 2018). For instance, the western part of the Moesian Platform contains Carboniferous igneous structures (Paraschiv, 1979) poorly documented. Another example is the Teisseyre–Tornquist Zone (TTZ, Figure 1a), which represents a transition between the thick crust of the East European Craton (EEC) and the thinner crust of the Palaeozoic Platform to the SW (Mazur et al., 2016). For a long time, TTZ has been considered a fossil plate boundary of the EEC corresponding to the limit of early

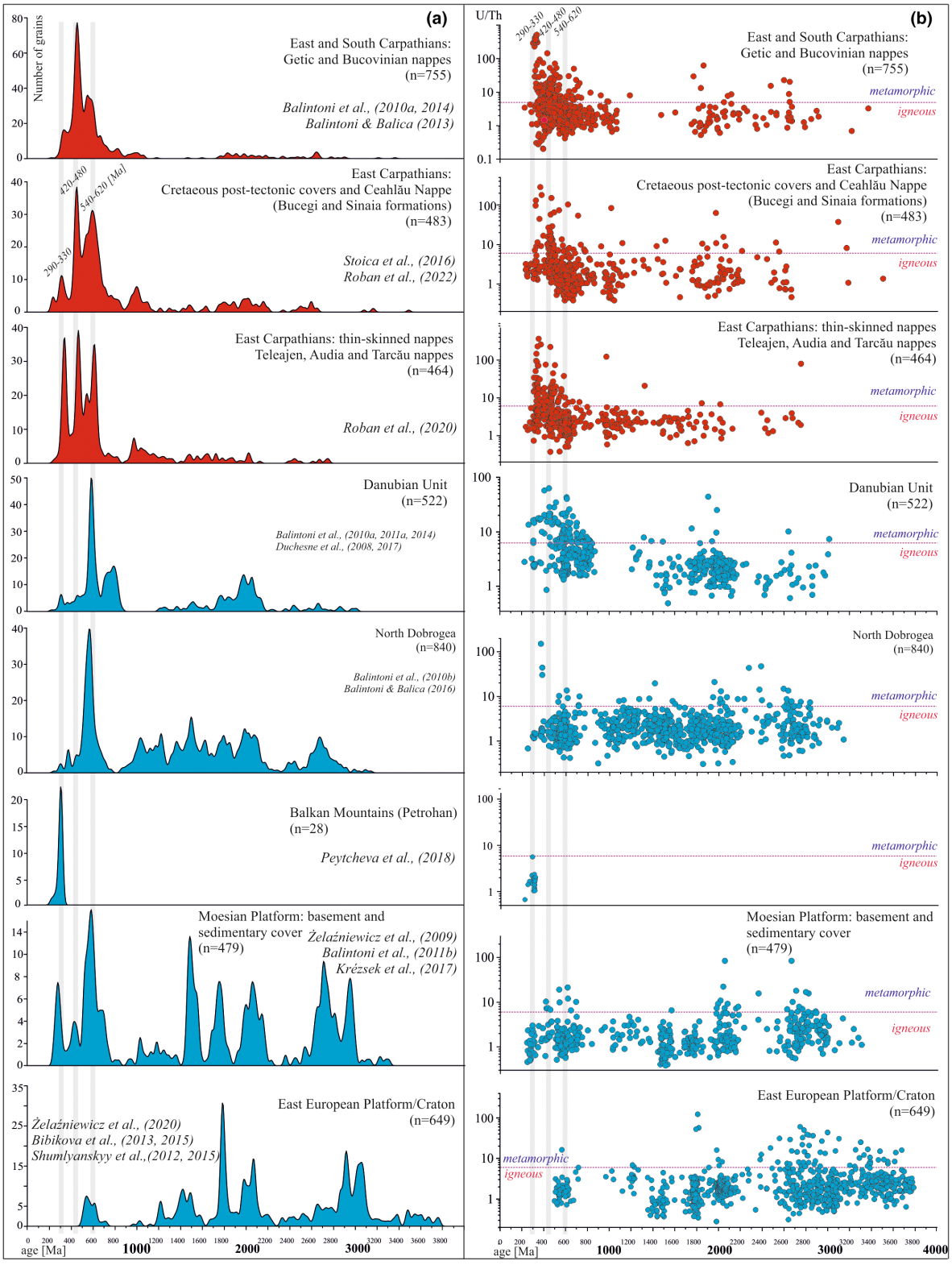

FIGURE 6 (a) KDE (*Kernel Density Estimate*) age probability diagrams corresponding to Carpathian and foreland zircons, compiled from various published sources; (b) U/Th ratios of the samples used for DZ. U/Th < 5 are of igneous origin. Internal Dacia mega-unit and accreted units (Ceahlău and internal thin-skinned nappes) are with red lines and dots. Foreland units, North Dobrogea and the Danubian Unit are shown in blue.

Palaeozoic palaeocontinent Baltica. The new geophysical data suggest the continuation of the Precambrian basement of the EEC and its Lower Palaeozoic cover towards the SW underneath the Palaeozoic Platform. Moreover, Krzywiec et al. (2017) found that the Pre-Permian deposits overlying the thinned Eastern European basement, along the TTZ, were involved in Variscan shortening. Notably, the Oligocene deposits are absent in the foreland units, either due to erosion or lack of deposition (Saulea et al., 1969). U–Pb ages and U/Th rations provided by zircons (Figure 6a,b) within the European units are different from the ones corresponding to the Dacia mega-unit. The post-Variscan age signatures (245–310 Ma) of the Danubian Unit (Balintoni, Balica, Seghedi, et al., 2010, 2011; Balintoni et al., 2014; Duchesne et al., 2008, 2017) and the ones of North Dobrogea (248–310 Ma—Balintoni & Balica, 2016; Balintoni, Balica, Seghedi, et al., 2010) are indicated by post-collisional granitoids found in the Peri-Gondwanian basement (Von Raumer et al., 2013). Similar age signatures are found in magmatic intrusions within the Balkans (Carrigan et al., 2005; Peytcheva et al., 2018) and the Bohemian Massif (Tichomirowa et al., 2019). The dominant ages of the Danubian Unit and North Dobrogea lie within the 565–585 Ma interval, while the overall age frequencies display a general decrease towards 800 Ma (Balintoni, Balica, Seghedi, et al., 2011; Balintoni et al., 2014). The Danubian unit is characterized by a metamorphic sequence derived from c.800 Ma old protoliths of island arc origin that were intruded by Neoproterozoic plutons (Liégeois et al., 1996). Furthermore, ages >1 Ga are quite abundant within the Moesian Platform (Balintoni et al., 2011; Krézsek et al., 2017; Żelaźniewicz et al., 2009) and North Dobrogea (Balintoni & Balica, 2016). The exposed basement in the Ukrainian Shield contains zircons that yield mainly Proterozoic and Neo-archean ages (c. 1500, 2000 and 2700 Ma, Bibikova et al., 2013, 2015; Shumlyanskyy et al., 2012, 2015). This signature is also recognizable in the western Neo-proterozoic sedimentary cover of the East European Craton (Francovschi et al., 2021; Roban et al., 2020; Żelaźniewicz et al., 2020).

3 | DATA AND METHODS

We analysed five key outcropping sections of the Fusaru and lower Kliwa formations from Tarcău Nappe (Supporting Data SD 1): Fusaru North (FN), Fusaru South (FS), Kliwa North (KN), Kliwa South (KS) and Kliwa-Fusaru South (KFS) (Figure 2). Each section measuring about 20–30 m, was evaluated by using standard sedimentological techniques (SD 1). The facies analysis workflow (Miall, 2000) used lithologies for separating each individual facies and interpreting depositional hydrodynamic regimes (Lowe, 1982; Mulder & Alexander, 2001) followed by mapping of sequences in terms of architectural elements specific to deep-water systems (i.e. channels, levees and splays/lobes) (Posamentier & Walker, 2006). Four to six shale samples were collected from each section for calcareous nannofossils age dating (SD 2). The nannofossil biostratigraphy follows Gradstein et al. (2004). Four to six sandstone samples were collected from each studied section for determining their petrographical composition (SD 3). The method used involved a quantitative analysis of 28 thin sections (i.e. point counting method). This method allows the determination of petrographical signatures that correspond to various tectonic facies by plotting the results of the quantitative analysis in ternary diagrams (i.e. Dickinson, 1985; Garzanti, 2019).

The U–Pb detrital zircon dating (SD 4) was undertaken on four samples, two from the quartzous Kliwa sandstone and two from the lithic Fusaru sandstone. For this purpose, 3 kg from each sample were crushed and sieved to separate the <300 μm fraction. The <300 μm heavy mineral mass was separated with a high-density liquid (diiodomethane with 3.3 $g cm^{-3}$ density), followed by a further magnetic separation using a Frantz Magnetic Barrier Separator. The separated zircons were mounted in epoxy resin along with other zircon specimens of known age. The U–Pb isotopic analyses were performed on polished individual grains using laser ablation at the Arizona LaserChron Center, on an Element2 high-resolution single collector inductively coupled plasma-mass spectrometer (LA-ICP-MS) equipped with a 193 nm Excimer laser with a beam diameter of 30 μm (Gehrels et al., 2008). The random selection of 100 crystals ensured an analysed sample representative of the entire zircon population (Gehrels, 2014). Every five crystals of unknown age are bracketed by a known standard (SD 4); our primary standards for this study were Sri Lanka and R33 zircons, which have ages similar to most of our unknowns. Ages that are <90% concordant (discordance between $^{206}Pb/^{238}U$ and $^{207}Pb/^{235}U$ ages) were discarded from further analysis. For ages younger than 1.4 Ga, the $^{206}Pb/^{238}U$ age was reported and used, whereas for ages older than 1.4 Ga, we use the $^{206}Pb/^{207}Pb$ age. The obtained results were plotted by IsoplotR using the same Kernel bandwidth (15) and histogram binwidth (15). Maximum Likelihood Estimation (MLE) was used to evaluate the maximum depositional age (SD 5) of sedimentary formations (Vermeesch, 2021).

4 | RESULTS

4.1 | Sedimentology and stratigraphy

The analysed sections (Figures 5 and 7) enclose sandstone bodies, some with thicknesses in excess of 10 m, alternating with packages composed of grey and black shales with

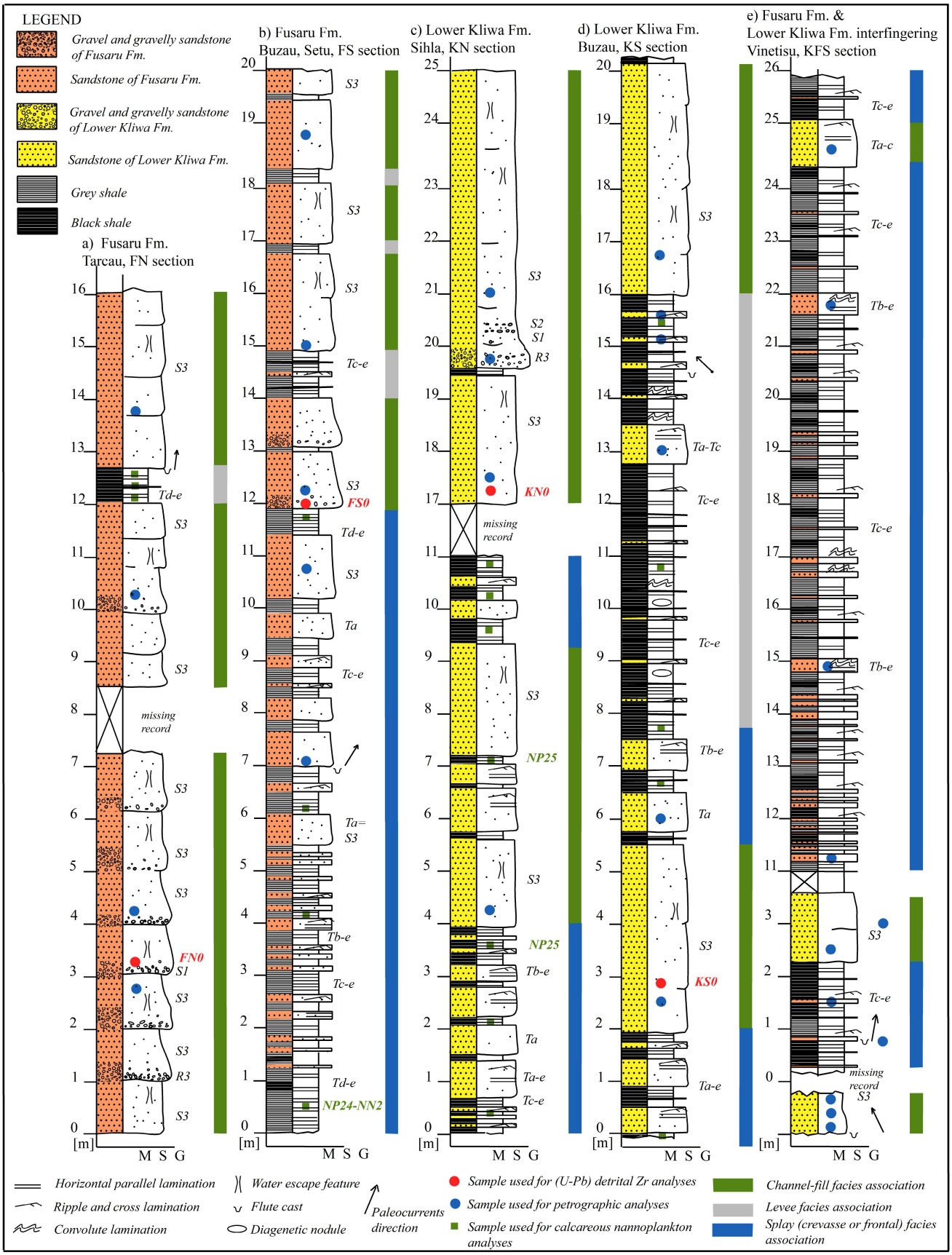

FIGURE 7 Sedimentological characteristics of the measured sections for Fusaru Formation (a,b); Lower Kliwa Formation (c,d), and the interfingering zone (e).

silt or cm-thick sandstones. According to the result of the calcareous nanoplankton analysis (SD 2), all sections belong to the upper Oligocene (upper Chattian) depositional interval (NP25-NN1 biozones), except the FS section (Figure 5), where the Fusaru Formation reaches the lower Aquitanian (NN1-NN2 biozones).

4.1.1 | Sedimentary facies

In the measured sections (Figure 7), facies specific to high density (*R2, R3, S1, S2, S3*, Lowe, 1982) and low-density turbiditic currents (*Tb-e*, Bouma, 1962) were identified. In the case of high-density turbiditic currents (9%–35% volumetric sediment concentration), the main sediment support mechanism is turbulence, however, higher sediment concentrations near the base of flows are supported by grain-to-grain interactions (Lowe, 1982; Mulder & Alexander, 2001). Normally graded gravelly sands (*R3*) or sands (*S3*) are the result of settling from the dense turbulent body (Figure 8a), while laminated facies suggest deposition from traction carpets (*S2*, Figure 8b). In the case of low-density turbiditic currents, a fining upward bed comprising five terms (*Ta-e*), or sometimes part of the five terms of succession, express the progressive decrease in current density and tractive power. The *Ta*, (Bouma, 1962) is equivalent to the *S3* facies (Lowe, 1982) and it is thought to be a high-density component, while the final term (*Te*) is an expression of the fine sediment settling from the turbulent suspension cloud, together with hemipelagic and pelagic sediments (Figure 8c,d). In addition to the classical turbiditic facies, Sylvester and Lowe (2004) described the outcrop located in the immediate vicinity of the FS section (Fusaru Formation), indicating the presence of hybrid facies resulting from slurry flows.

4.1.2 | Facies associations

Meters thick sandy facies with common erosional/sharp base beds (*S1-S3*, secondary *R3, S2*) and a fining upward tendency, are interpreted as channel-fill deposits (CH) (Figure 7). The deposits dominated by fine facies (*Td-Te*, with *Tc* intercalations) are interpreted as levee (LV) deposits that are genetically related to channel-fill deposits. The coarsening and thickening upward sequences (expression of progradation) suggest frontal splay (lobe; FrS) or crevasse splay architectures (CS). When the levees of meandering channels are broken due to higher energy flows, crevasse splays or lateral lobes can form. The lateral or frontal splays or channel complex deposits are formed in the distal part of the leveed channel systems (Posamentier & Walker, 2006).

4.1.3 | Fusaru formation

The northern section FN (Figure 7a) shows channel-fill features, containing incomplete and amalgamated beds (Lowe, 1982). The amalgamated units up to 12-m-thick dominated by gravelly sandstone (*R3*) and sandstones (*S3*), displaying water-escape structures were interpreted as high-density flows deposited in channels. The gravel clasts range between granules and pebbles at the base of beds (Figure 8a,e). The 0.7 m thick, fine-grained dominated facies intercalation (*Td-e* beds) with bituminous shales and silts are interpreted as deposited from suspension and could represent the inter channel-levee deposits. Flute casts indicate an NNE palaeoflow direction (Figure 7a). The southern FS section (Figure 7b) shows a coarsening and thickening upward tendency, interpreted as the transition from splay associations to channel-fill deposits and levees, consisting of grey and bituminous shales alternating with low-density unconfined turbidites. In FN and FS sections, the sandy facies often preserve flute and bounce casts on the soles of the beds. The measurements (60 degrees azimuth) confirmed the directions of palaeocurrents mainly towards the present-day NE (Figure 7b) according to (Contescu et al., 1966). These authors found that the thick Fusaru sandstone layers (channel deposits) have a predominantly northern direction, while the thinner beds (splay and levee deposits) have a more variable palaeoflow orientation towards NW and NE.

4.1.4 | Lower Kliwa formation

The northern KN section (Figure 7c) shows a general thickening upward trend. In the first 11 m, dm thick sandstone beds (*Ta/S3* facies), alternating with cm thick sandstones (*Tb-Tc*) and bituminous shales, are interpreted as splay deposits. The top of the sequence is characterized by channel-fill associations dominated by amalgamated *S3* facies. Tractive facies (*S1* and *S2* facies containing pebbles and granules; Figure 8b) was identified towards the top of the section. Calcareous nanoplankton associations were assigned to the NP25-NN1 biozones (SD 2). The southern section KS (Figure 7d) is interpreted to be an alternation of channel-fill (dominated by sandstones) and levees (Figure 8f) composed of bituminous shales (*Te*) and thinner sandstone intervals (*Tb-Tc*).

The Oligocene deposits from the Vineţişu Valley, in the South East Carpathians, are over 850 m thick (Figure 5). The lower 500 m exposes bituminous shales overlayed by Kliwa sandy Formation, while the upper 350 m shows features of Fusaru Formation (Ştefănescu et al., 1993, 2018). The KFS (Figure 7e) describes the upper part of the Fusaru

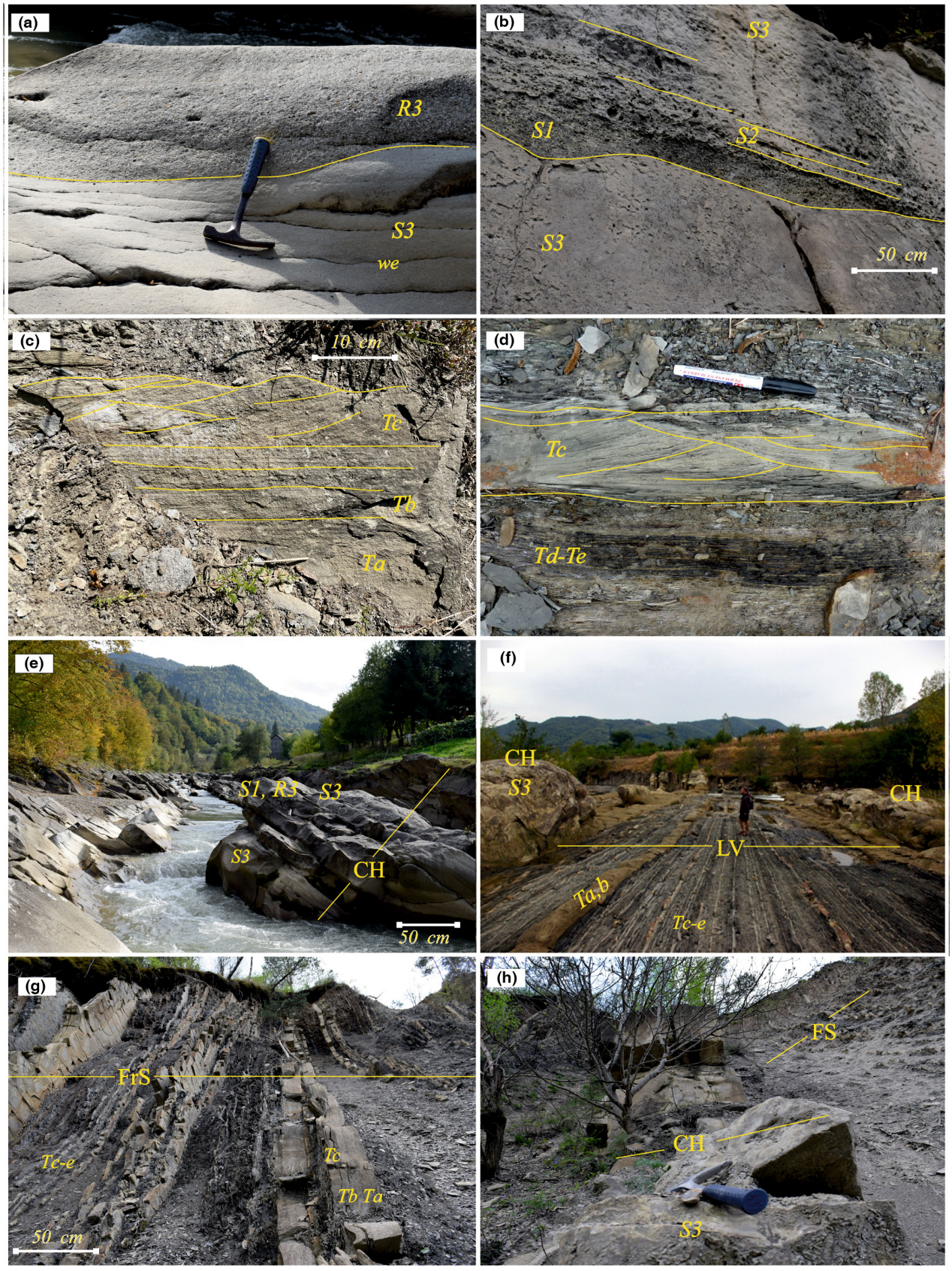

Formation where the alternation of cm to dm-thick lithic sandstones (*Ta-c*) with grey and black shales (*Td-e*) and marls could suggest distal frontal splay and possibly basin plain facies (Figure 8g). Palaeocurrent measurements of the Fusaru sandstone beds indicate a NE direction (Figure 7e). A few smaller Kliwa channel-fills embedded

FIGURE 8 Individual facies and facies associations of the analysed sedimentary formations. (a) Erosional boundary between facies *S3*—normally graded sandstones with water escape (*we*) structures, and facies *R3* (Lowe, 1982)—normally graded conglomerates (pebbles and granules). Fusaru Fm., FN section; (b) Normally graded gravelly sandstone (*S1*) and stratified gravelly sandstone (*S2*) intercalated between *S3* facies. Lower Kliwa Fm., KN section; (c) The Bouma bed has the first three divisions: normally graded sandstone (*Ta*), parallel horizontally laminated (*Tb*) and cross-laminated sandstone (*Tc*). Fusaru Fm. near the FS section. (d) Fine turbiditic facies (*Tc-e* divisions; Bouma, 1962) identified between thick sandstone levels. Lower Kliwa Fm., KS section; (e) Channel-fill (CH) association specific to the Fusaru Fm., FN section. Mainly *S3* facies in alternation with *S1* and *R3*. In this location, fine facies are rare; (f) Levees (LV) association, specific to the Kliwa Fm., KS section, consisting of the finest facies (*Tb-Te*, Bouma). The association lies between channels of metric thickness; (g) Frontal splay association (FrS), Fusaru Fm., KFS section; (h) Kliwa channel embedded in frontal splay associations and possible basin plain facies specific to the Fusaru Fm., KFS section.

in the Fusaru Formation were identified based on their lithological character and NW palaeocurrent direction (Figure 8f). This lithostratigraphical relationship suggests an interfingering zone between the Kliwa and Fusaru formations in this area.

4.2 | Petrology

4.2.1 | Fusaru formation

The samples from the northern (FN) and southern (FS) sections show similar textural and compositional features in thin sections (SD 3). The grain size generally ranges between medium and coarse sands but gravels can be identified as well. The sandstones are texturally immature, displaying poor sorting and a subangular to subrounded contour. Matrix (Figure 9a) dominates the coarser facies (i.e. gravelly sandstones) and is composed of clay minerals, while carbonate cement is present within sandstone facies. Metamorphic lithoclasts are dominant (i.e. gneiss fragments and schists; Figure 9b) and are lithologically similar to metamorphic rocks found in the Getic and Bucovinian nappes (Roban et al., 2020 and references therein). Sedimentary lithoclasts (i.e. micritic limestones, siliciclastic claystone and siltstone fragments) were also identified, along with weathered volcanic rock fragments (Figure 9c). Well-preserved vesicular volcanic glass fragments were found (Figure 9d). In addition, the analysed samples contain monocrystalline (Qm) and polycrystalline quartz (Qp), mica and feldspar granoclasts. The Qm/Qp ratio varies between 0.5 and 1.5, arguing the immature character of these sands. According to the classification of Garzanti (2019), the analysed samples are litho-quartzose and feldspatho-litho-quartzose arenites (Figure 10a). After McBride (1963), the rocks are (sub)litharenite/(sub)feldspathic litharenites (Figure 10b). If the matrix exceeds 15% the sandy rocks are lithic wackes (sensu Dott, 1964). Plotting the relevant clast proportions on tectofacies ternary diagrams indicates that a recycled orogen (QtFtLt diagram, Figure 10c) or a recycled transitional orogen (QmFtLt+Qp diagram, Figure 10d) might be a potential source area.

4.2.2 | Lower Kliwa formation

The samples are fine sandstones (average = 0.125 mm) which are better sorted than Fusaru Formation. The grains are more rounded, although populations with different degrees of roundness were observed (Figure 9e,f). The proportion of quartz granules reaches 98%, and the monocrystalline category is dominant. Qm/Qp ratio (SD 3) suggests a very high textural maturity. Secondary feldspar and mica granules were identified. The gravelly *R3* facies from the base of the KN section (Figure 7c) contains a large proportion of low-grade green metamorphic lithoclasts (granules and pebbles) and a well-sorted quartz-rich matrix cemented with calcite and silica (Figure 9g). Another characteristic is the presence of authigenic glauconite granules. The sandy clasts are held together by siliceous cement (Figure 9f), which is sometimes pigmented with iron oxides (Figure 9g). In general, the samples are quartz arenites (Figure 10a,b). Note that the thicker sandstone beds (i.e. channel-fills) are well-sorted and free of matrix, containing grains bonded exclusively by siliceous cement, while the thinner layers (levees and splays) contain carbonate cement, in addition to a higher matrix content (Figure 9h). The tectofacies classification mainly indicates a cratonic source area (Figure 10c,d).

Furthermore, seven petrographical samples from the KFS section at Vineţişu Valley (Figure 7e) indicate that three samples belong to the Kliwa Formation, located at the base of the section, while the other samples have Fusaru sandstones characteristics (Ştefănescu et al., 1993). The petrographical analyses separate the quartzous character of the Kliwa sandstones and the predominantly lithic composition of the Fusaru sandstones and suggest the interfingering of the two petrographically distinct sandstone types. The samples collected from the Kliwa-type channel found in the Fusaru Formation (Figure 7e) confirm the quartzose composition. This demonstrates that at times Kliwa quartzous sand dominated deposition in the overall Fusaru depositional environment and the interfingering of the two different types of sediments in the deeper part of the basin. In addition to the main craton source for the Kliwa samples in sections KS, KN and KFS, the

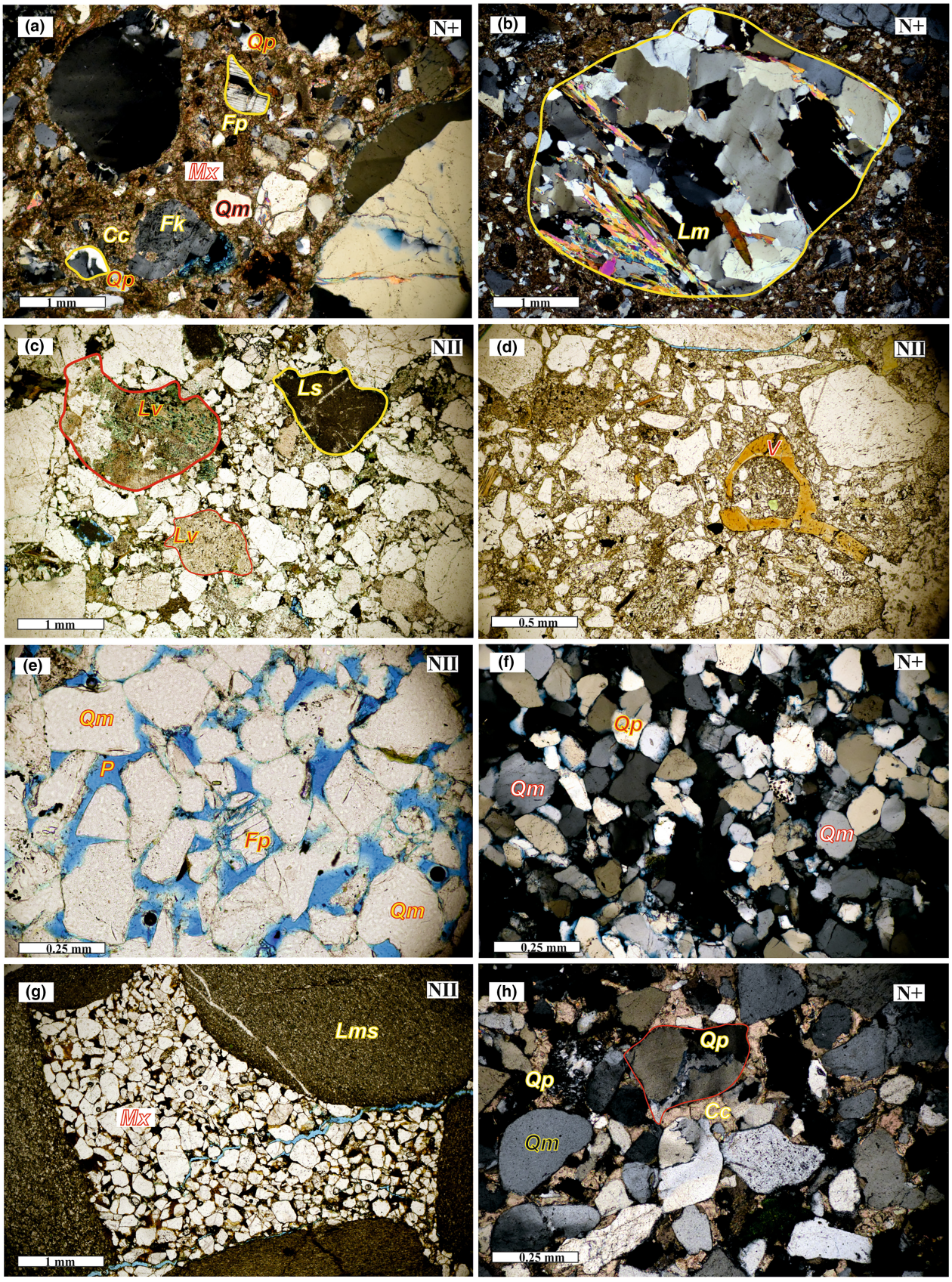

recycled quartz orogen (Figure 10d) is supported by the polycrystalline quartz granules and the green fragments. Some Kliwa samples in the KFS section appear to have more matrix, mica and metamorphic lithoclasts (SD 3), suggesting a mixture of the two types of sands (Fusaru and Kliwa).

FIGURE 9 Thin section images illustrating the petrography of Fusaru and Kliwa sandstones. (a) General aspect of Fusaru sandstone: polycrystalline and monocrystalline quartz and plagioclase feldspars granoclasts. Phyllosilicate and carbonate matrix and cement. Poor sorting, FN locality; (b) Metamorphic fragment surrounded by a phyllosilicate matrix, FN locality; (c) Volcanic, sedimentary and metamorphic lithoclasts, FS locality. Top left: volcanic lithoclast with a feldspar phenocrystal that has undergone clay and carbonate replacement processes. In the centre of the image: volcanic lithoclast with plagioclase feldspar crystals, FS locality; (d) Vesicular vitroclast displaying a well-preserved structure, FN locality; (e) Typical Kliwa facies: well-sorted quartz sandstone with an intergranular porosity of 15%–20%. In the centre: a plagioclase feldspar granoclast, KN locality; (f) Quartzose sandstone with a predominantly siliceous cement. Monocrystalline quartz granoclasts with different degrees of roundness, from angular to rounded, are dominant, KS locality; (g) *R3* facies, Kliwa sandstone, KN locality. Metasedimentary lithoclasts (silt and clays weakly metamorphosed in the greenschist subfacies). These fragments are bounded by a matrix resembling the typical Kliwa quartz arenite, with siliceous and ferruginous cement; (h) Quartzous sandstone, *Ta* facies, KS locality. The quartzous composition and carbonate cement are noticeable. Cc, carbonate cement; Fk, potassium feldspar; Fp, plagioclase feldspar; Lm, metamorphic rock fragment; Lms, metasedimentary lithoclast; NII, parallel nicols, N+, crossed nicols; P, porosity; Qm, monocrystalline quartz; Qp, polycrystalline quartz; V, vitroclast.

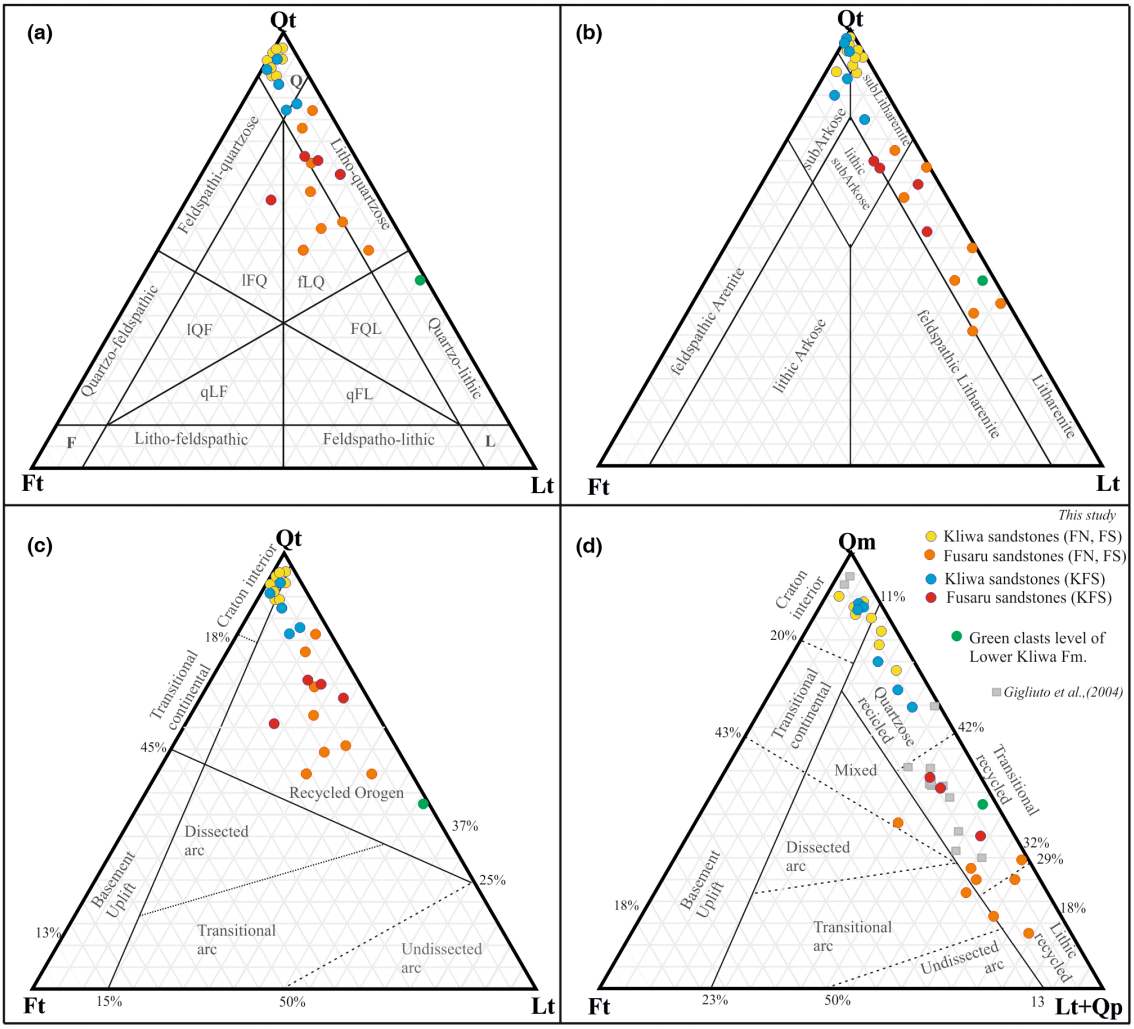

FIGURE 10 Petrographical data plots. (a) According to Garzanti (2019) classification, Kliwa sandstones are quartzose and Fusaru sandstones are lithic and feldspatho-litho quarzose; (b) The classical classifications (McBride, 1963) show that quartzose arenite and subordinate sub-feldspathic or sub-lithic arenite are typical for Kliwa samples while Fusaru sandstones is characterized by litharenite; (c) QtFtLt diagram of Dickinson (1985), shows the tectonic framework of an inner craton (Kliwa sandstones) and recycled orogen (Fusaru sandstones); (d) QmFt Lt + Qp diagram (Dickinson, 1985) suggests a craton interior and quartzose recycled orogenic fields: recycled quartzose for Kliwa sandstones and transitional to lithic recycled orogen fields for Fusaru sandstones.

4.3 | Detrital zircon geochronology

Two samples collected from the Fusaru Formation show similar U–Pb (DZ) age distributions and U/Th patterns, and they are different from the ones identified in the two samples from the Kliwa Formation (Figure 11a,b).

4.3.1 | Fusaru formation

The samples (FN0 and FS0) acquired from the analysed sections (Figure 7a,b) display an age spectrum spanning between 21.3 and 2893 Ma (Figure 11a), with the highest peak corresponding to the Ordovician (c. 450 Ma). The peaks become less pronounced, recording values in the Neo-proterozoic (c. 600 and c. 765 Ma). The age distribution profiles resulting from KDEs for the two Fusaru samples are similar to the ones displayed by zircons from the Getic and Bucovinian thick-skinned nappes (Balintoni et al., 2014) and the inner thin-skinned nappes (Roban et al., 2020; Stoica et al., 2016), (Figure 6a,b). One age cluster that peaks at 290–330 Ma can be associated, based on zircon U/Th ratios (Figure 11b), with two possible sources: a magmatic (U/Th < 5) and a metamorphic (U/Th > 5), (Hoskin & Schaltegger, 2003). This characteristic is also found in rocks from the Ceahlău (Roban et al., 2022), Teleajen, Audia and Tarcău nappes (Roban et al., 2020), suggesting a mix between magmatic and metamorphic sources derived from the Dacia and the Danubian units (Figure 6b). Another shared a peak at 72 Ma (Late Cretaceous, Campanian stage) is attributed to subduction magmatism associated with the nearby closure of the Neotethys (Gallhofer et al., 2015). Lastly, the two Fusaru samples reveal two intriguing peaks at ~25 Ma which are less noticeable than the Cretaceous ones, albeit still distinctive. Maximum Likelihood Estimation (Vermeesch, 2021) at 22.22 ± 0.20 Ma, in the Early Miocene, was found in the FS section (SD 5), and it might be the youngest depositional age of the Fusaru Formation. These data confirm the results of the calcareous nannofossils analysis indicating that the top of the Fusaru Formation is younger than the top of the Lower Kliwa Formation. The youngest zircons are probably linked to vitroclasts and lithic fragments of volcanic origin contained in the Fusaru Sandstone, which are confirmed in thin sections. Their presence is not surprising since some of the earliest manifestations of regional calc-alkaline magmatism (typically tuffs and other forms of explosive magmatism of rhyo-dacitic compositions) are late Oligocene to early Miocene in age (Cvetković et al., 2007; Vlăsceanu et al., 2021 and references therein).

4.3.2 | Lower Kliwa formation

The samples (KN0 and KS0) acquired from the analysed sections (Figure 7c,d) show a broader age range (i.e. from 114 to 3250 Ma). One distinctive feature is the dominance of grain clusters with ages >800 Ma. Additionally, these ages, including those >800 Ma, are possibly derived from foreland units (Moesian Platform, Eastern European Platform/Craton and North Dobrogea; Figure 6a,b). Cambrian–Neo-proterozoic ages (c. 500–570 Ma) were identified in the sedimentary cover of the East European Platform (Francovschi et al., 2021). The c. 430–670 Ma age cluster could represent internal sediment sources corresponding to the Getic and Bucovinian domains. Most notable are the peaks of Carboniferous age (c. 300–320 Ma) within the KS0 sample (Figure 11a,b). The zircons yielding these ages have a U/Th ratio < 5 (Figure 11b), suggesting a magmatic origin specific to Variscan post-collisional granitoids within the foreland units Moesian Platform, Danubian Unit and North Dobrogea and possibly the Balkan and Sredna Gora units (Balintoni et al., 2014; Carrigan et al., 2005; Duchesne et al., 2008, 2017; Jovanović et al., 2019). This Carboniferous age cluster is absent from the KN0 sample (Figure 11a,b), and a similar situation is encountered in the case of Albian sediments enclosed by the Vrancea Nappe on the same northern alignment (Roban et al., 2020). Furthermore, the zircons contained in the KN0 sample, which are associated with a Permian peak (265 Ma), could be sourced from North Dobrogea magmatic intrusions (Balica, unpublished zircon U–Pb data).

5 | DISCUSSION: PROVENANCE AND SEDIMENTARY ROUTES

The integration of the new sedimentological, biostratigraphical, petrological and DZ U–Pb geochronological data and existing palaeo-tectonic reconstructions (Barrier et al., 2018; Van Hinsbergen et al., 2020) and lithofacies maps (Popov et al., 2004; Saulea et al., 1969), allowed us to reconstruct the sedimentary routes of the Oligocene–lower Miocene depositional interval. During this time, the Moldavides foreland basin was shortened as the Carpathian Orogen advanced over the East European, Scythian and Moesian platforms; after the consumption of the Ceahlău oceanic domain, which led to continental collision starting in the Eocene (Necea et al., 2021 and references therein). By this time, the Getic-Bucovinic (Dacia) units and part of the Cretaceous wedge (Ceahlău) were already exhumed, forming the active western margin of the Moldavides foreland basin (Figure 12a,b). The Moldavides basin

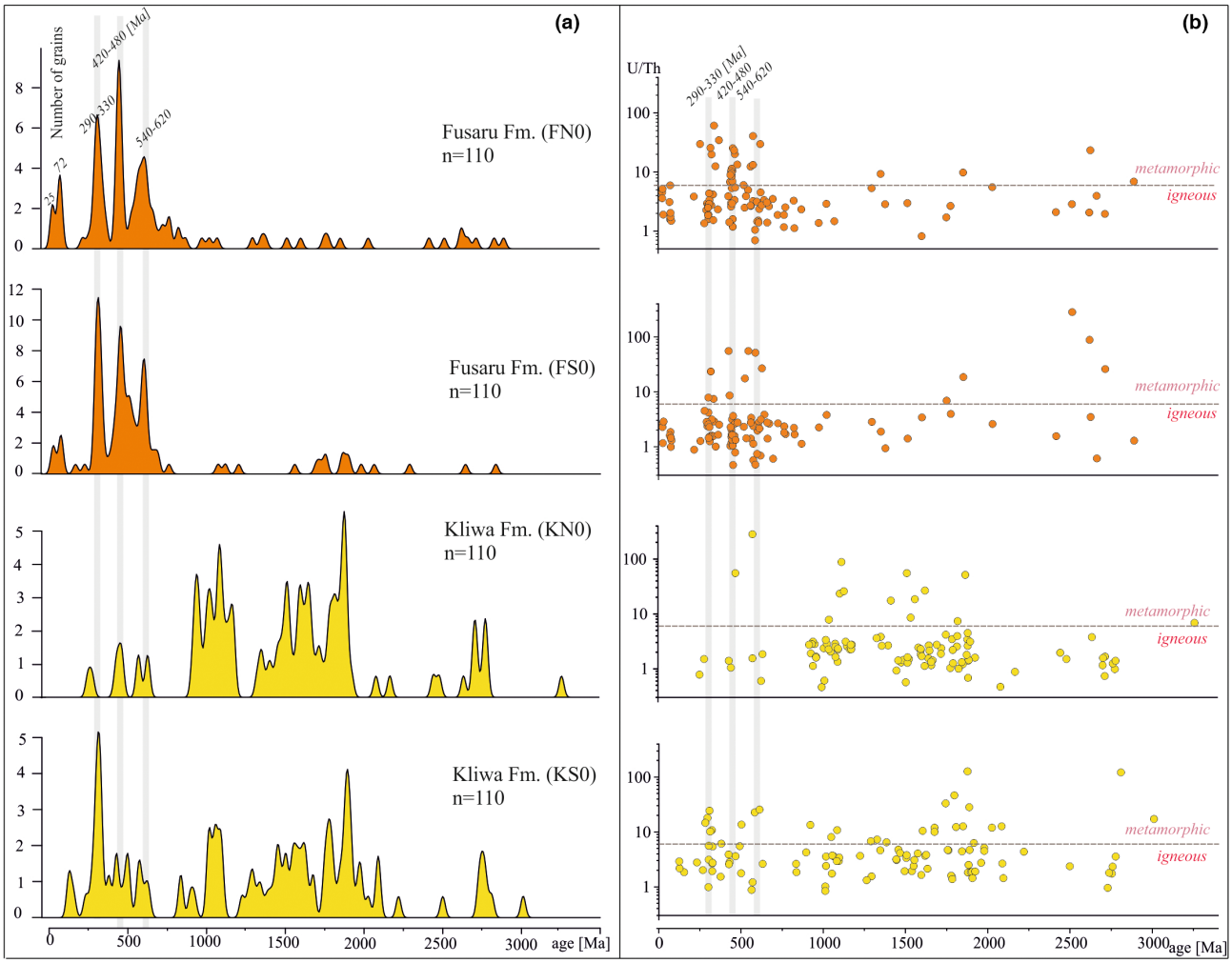

FIGURE 11 (a) Age distribution of U–Pb ages determined on detrital zircons. (b) U/Th ratios of the analysed samples. From each sample, 110 detrital zircons were analysed. The age distribution of Fusaru detrital zircons (orange) is markedly different from that of Kliwa sandstone zircons (yellow).

was narrow and asymmetric, with an NW-SE oriented axis, a 250 km width (Roure et al., 1993), and an 800 to 900 km length, considering its continuation to the NW, stretched from the Moesian Platform to the Bohemian Massif, and has different names (see Oszczypko, 2006 for regional reconstructions and different local names of the units). The maximum water depth of 1000 m was established based on microfaunas of the Rupelian Lower Dysodiles and Lower Menilites (Figures 4 and 5) containing benthonic foraminifers (genus *Cyclammina, Chilostomella*, *Eponides*; Książkiewicz, 1975 and references therein) and fish remains (i.e. *Argyropelecus* sp., *Scopeloides* sp., see Bădescu, 2005 and references therein). The benthonic foraminifera (i.e. *Rhabdamina abyssorum*, see Bădescu, 2005; *Bulimina elongate*, see Książkiewicz, 1975) discovered in the Fusaru and lower Kliwa formations suggest an average water depth between 200 and 700 m (Bădescu, 2005). Feeding the Kliwa and Fusaru depositional systems, two main sources of clastic material located in the eastern and western parts of the basin and an additional southern source were identified (Figure 12a).

The *Kliwa depositional* system was active during the late Rupelian-late Chatian time interval and contains high-density turbidites forming amalgamated channels (1 to 15 m thick) in alternation with low-density turbidites, levees and distributary frontal or crevasse splay facies associations. Palaeocurrent measurements suggest an NW direction. The high quartz content and textural maturity of the Kliwa sandstones fit the East European Platform/Craton origin suggested by the tectofacies of Dickinson (1985). This is additionally supported by palaeocurrent measurements (Contescu et al., 1966, this study) and by detrital zircon ages well over 1 Ga (Figure 11a,b), common for rocks of the East European Platform/Craton (i.e. Bibikova et al., 2015; Francovschi et al., 2021; Shumlyanskyy et al., 2015). These characteristics and the presence of green clasts (e.g. Roban et al., 2020) place

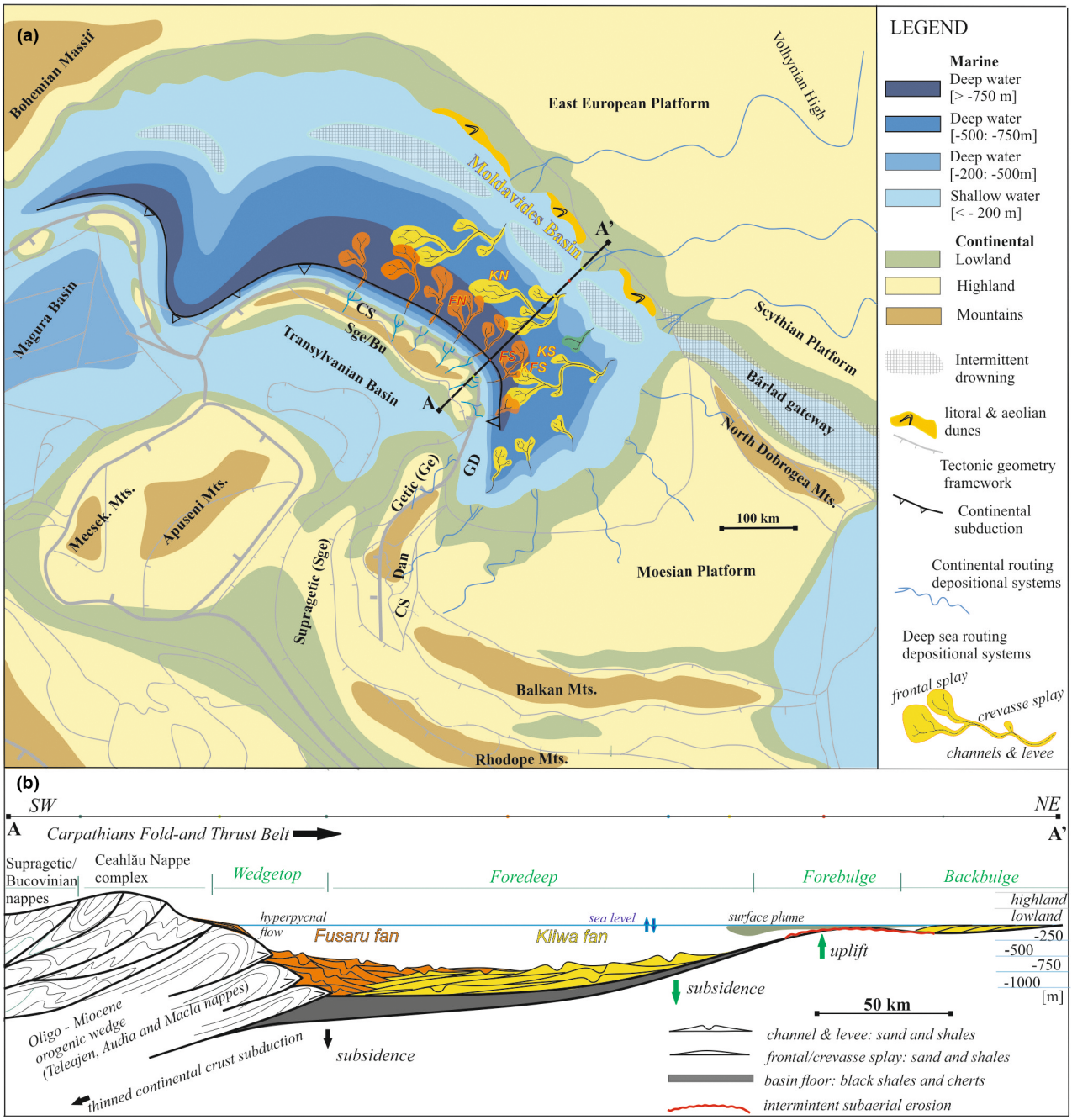

FIGURE 12 (a) Palaeogeographical reconstruction during Oligocene illustrating the possible drainage routes associated with the depositional systems Fusaru and Kliwa, as well as the turbidites morphology in the Moldavides Basin, based on the integration of the current study results and the previous comprehensive studies: litho-stratigraphical (Kovác et al., 2017; Popov et al., 2004; Salata & Uchman, 2019; Saulea et al., 1969) tectono-stratigraphical (Barrier et al., 2018; Van Hinsbergen et al., 2020—grey lines framework) and thermochronological (Fügenschuh & Schmid, 2005; Kounov & Schmid, 2012; Merten et al., 2010; Necea et al., 2021; Sanders et al., 1999). The turbidites system configuration has been interpreted based on sedimentological and palaeocurrents measurements acquired during this study and completed with those of (Contescu et al., 1966; Jipa, 1966); (b) Sketch showing the basin configuration during Oligocene-Miocene times, illustrating the advancing of the Carpathian indenter over the subducting plate. The basin depth is estimated based on micropalaeontological studies (see Bădescu, 2005 for more references). The active Western margin is dominated by the Fusaru system, which supplies the basin with lithic sand from the uplifted and eroded Getic-Bucovinian basement and the Cretaceous accretionary wedge; the Kliwa system feeds the basin with quartz-rich sand from the Eastern European Platform. A minor input is supplied by southern domains, (Moesian Platform, North Dobrogea Orogen or even the Balkan Orogen). The reconstruction does not extend further than Romania's border with Ukraine and Poland due to data availability. CS, Ceahlău-Severin Unit; Dan, Danubian Unit; FN, Fusaru North; FS, Fusaru South; GD, Getic Depression; Ge, Getic Unit; KN, Kliwa North; KS, Kliwa South; Sge, Supragetic Unit; KFS-Kliwa-Fusaru South is the location of the analysed sections on this reconstruction.

the Kliwa depositional system on the eastern margin of the Moldavides Basin, specifically the foredeep and forebulge depozones. The quartz enrichment of these sandstones can be the result of (i) weathering processes (e.g. Lorentzen et al., 2020; Suttner et al., 1981) during clast transport through long river systems (>400 km) across the East European Platform (Figure 12a), or (ii) multiple deposition-erosion recycling stages, as suggested by high Qm/Qp ratios (SD 3). The abundance of metamorphic polycrystalline quartz grains indicating quartz recycled orogenic tectofacies for some Kliwa samples raises the question of whether recycled or peneplenized orogens may be present in the western margin of the East European Craton in addition to batholiths. Processes such as hypopycnal flows (e.g. Sømme et al., 2009) associated with deltaic deposition on the wide shelves of the East European and Scythian platforms could have contributed to the sorting of the Kliwa sandstone by separating low-density fine sediments (surface plume) from higher density coarser sand. Wave action is another possible sorting agent that involved the reworking of deltaic sands, however, to what extent this basin was subject to high wave energy remains unknown, since making any assumptions in this regard would partly require an analysis of Oligocene shallow-marine deposits. Nevertheless, longshore currents could have led to the development of strandplains, where aeolian dunes usually form. Quartz enrichment is sometimes attributed to sand reworking by aeolian processes. However, the presence of aeolian deposits, as well as their extent (local, restricted to strandplains or regional, extending further inland) are uncertain. Sediment transport to the shelf edge during forced regressions and related gravity flows led to the transport and deposition of deep-water sand. During the turbidity flows sand is concentrated in the lower part of the flow where it is confined by channel walls (Posamentier & Walker, 2006). Meanwhile, finer sediments travel unconfined in the upper part of the flow and are shed out of the flow-through spills over levees. This is the main mechanism that separates channel-fill clean sands from finer deposits of thinly bedded sandstones and mudstones associated with levees and overbanks (Nilsen et al., 2007). The coarse green schist clasts identified in Kliwa channel fill (Figures 8b and 9g) suggest a more proximal source, and an intra-basin ridge located in the eastern part of the depositional system could source these clasts. A topographical ridge could represent the uplifted forebulge (Figure 11b), although assumptions related to the basin's flexural wavelength need to account for the subducting plate's flexural rigidity, which controls the lateral extent of the forebulge and the distance between its crest and the foredeep cratonic margin. Furthermore, Oligocene sediments are absent from the East European platform based on wells and palaeogeographical reconstructions in the context of the Late Cretaceous–Palaeogene inversion (Gedl & Worobiec 2020; Jarosiński et al., 2009; Krzywiec & Stachowska, 2016), which indicates an uplifted area acting as a catchment for rivers flowing westward. Considering the shape of the basin and tectonic evolution it is convenient to assume that sediment accommodation in the Moldavides Basin was primarily controlled by tectonic forces rather than eustatic related to the flexure of the subducting plate (Rögl, 1999). The flexural subsidence as a result of orogenic loading and/or unloading cycles during the Oligocene is not well documented in this area, and even if tectonism might have been the primary control on deep-water deposition, the sea level changes would likely have a significant contribution to stratigraphy architecture. The early Oligocene records a slight rising of the sea level after a significant (60 m) fall at the Eocene–Oligocene boundary (Miller et al., 2020, Figure 4), as the effect of climate variability. At the Rupelian–Chattian transition, a second sea-level fall takes place, followed by a new rise during the main deposition interval of Kliwa and Fusaru systems. If the basin had been temporarily isolated and intermittently connected to the Global Ocean, then the Chattian Fusaru and Kliwa formations would have deposited during a more than 5 Ma extended highstand, obviously influenced by higher frequency and smaller amplitude sea-level cycles.

5.1 | The Fusaru depositional system

Developed on the western active basin margin during the late Rupelian–early Aquitanian (Figure 11a,b). We reconstructed a series of coalescent drainage systems connecting the source area with the deep-water sector of the basin through the wedge top depozone. In the foredeep depozone, the sediment routing directions take a sharp turn towards the north, parallel with the advancing orogen and along the basin axis, where the basin deep-water depocentre was most likely located (Figure 12a). The Fusaru sandstones undoubtedly have a Carpathian source based on the dominance of metamorphic rock fragments, palaeocurrent directions and abundance of Ordovician detrital zircons (Figure 11a,b), similar to those from the Bucovinian nappe basement and Cretaceous orogenic wedge (Figure 6a,b). The textural and compositional immaturity of the Fusaru sandstones suggests a short routing system, 50 to 150 km long, defined by a narrow shelf deeply incised by canyons, where high-energy and long-lived hyperpycnal flows fed deep-water fans (Sømme et al., 2009). The main control on basin accommodation within the foreland basin was the uplift of the Carpathian nappes pushed by the Dacia mega-unit indenter, coupled with high subsidence rates

in the foredeep basin due to orogenic loading underthrusted plate.

5.2 | The facies mixture zone

The interaction and interfingering of the Kliwa and Fusaru depositional systems in the central part of the basin is displayed in the KFS section. A thick package of stacked Kliwa channels, levees and frontal splays deposits are overlain by Fusaru frontal splays and basin plain deposits (Figure 7e), containing embedded Kliwa-type channels. A similar stratigraphy and petrography (see Figure 10d) are described 270 km north of our section by Gigliuto et al. (2004). A plausible cause for this stratigraphical relationship involves an initial stage of eastern Volhynian (Figure 12a) realm uplift, and a significative regression, which triggered the onset of the Kliwa deep-water system during the late Rupelian–early Chattian, prior to any major orogenic uplift. Subsequently, as the orogenic build-up led to increased exhumation rates along the western margin, the Fusaru system was initiated and prograded, eventually reaching the distal part of the Kliwa system during the late Oligocene–early Miocene, when intermittent sediment inputs from the east led to the interfingering of the two units. This hypothesis is supported by new biostratigraphical data on calcareous nannofossils (i.e. the NN2 biozone) and geochronological data (MLE at 22.2 Ma) which place the top of the Fusaru Formation in the Early Miocene. The Lower Kliwa sandstones contain detrital zircons of 460–430 Ma age, which proves the orogenic influence on the Fusaru depositional system. As an alternative, Ordovician zircons within the Kliwa sandstones might have been derived from a North Dobrogea (Figure 6) or recycled orogen of the edge of the East European Platform. The newly interpreted Variscan fold-and-thrust belt (Krzywiec et al., 2017) overlying the Teisseyre-Tornquiste Zone could have supplied Palaeozoic zircons and polycrystalline quartz, thus justifying the recycled orogen as a secondary source for the Kliwa sandstone (Figure 10c,d). Unfortunately, the U–Pb chronological data from the Variscan Fold and Thrust Belt (FTB) deeply concealed under the Romanian Carpathians area is not available at the moment to test this hypothesis. In contrast, the Fusaru sandstones do not contain convincing cratonic-derived zircons (e.g. >1 Ga). The basin floor interfingering of the deep-water fans can be speculatively explained by the alternation in sediment fluxes from one system to another with little sediment mixing by deep-water currents. Further evidence may be brought by subsequent geochronological studies on the interfingering areas along the nappes.

5.3 | The Southern depositional system

Late Carboniferous–Permian (320–265 Ma) detrital zircons of magmatic origin, collected from the southern sections of Kliwa and Fusaru outcrops (Figure 11a,b), suggest a sedimentary input from the Moesian Platform (Balintoni, Balica, Ducea, et al., 2011), North Dobrogea (Balintoni & Balica, 2016) or even the Danubian Unit (Balintoni, Balica, Seghedi, et al., 2011; Duchesne et al., 2017), hence sedimentary routes from these source areas towards the foredeep of the Moldavides Basin and the laterally-equivalent Getic Depression were suggested (Figure 11a). Some recent DZ analyses (Roban et al., 2022) show that the Danubian and Dacia units fed the Lower Cretaceous depositional systems of the Ceahlău-Severin Ocean (Sinaia Formation) with Variscan and post-Variscan magmatic and metamorphic zircons. These deposits were deformed during Late Cretaceous (Ceahlău Nappe), becoming later the recycled source for the Fusaru system, explaining the prominence of the 290–330 Ma peaks, especially in the FS section. Alternatively, the middle Eocene northward thrusting of the Balkanides over the Moesian Platform formed a narrow foredeep basin and an associated flexural bulge (Burchfiel & Nakov, 2015; Doglioni et al., 1996; Vangelov et al., 2013) which acted as a barrier preventing Balkan-derived sediments from entering the Moldavides Basin through river systems. This is supported by the presence of middle Eocene shallow marine sediments deposited on the Moesian Platform, at the bulge location (Vangelov et al., 2013). The lack of Oligocene deposits in the western part of the Moesian Platform can be linked to subaerial exposure and erosion leading to the formation of a large-scale northward drainage system. Within this system, canyons developed (Paraschiv, 1979; Tărăpoancă et al., 2004), transferring sediments towards the Moldavides Basin from the uplifted (during 44 to 30 Ma interval) Balkanides (Kounov et al., 2017). This could explain why detrital zircons associated with Carboniferous intrusions (Carrigan et al., 2005) in the West Balkans are present within the Fusaru and Kliwa South sandstones.

Fusaru-type small catchments and high-energy drainage systems can be found on the modern southern coast of the Black Sea (Pontides), where the shelf is narrow (Jipa et al., 2020). Modern Kliwa analogues of long drainage systems, crossing weathered cratonic areas and providing quartz-rich sands from both primary magmatic and recycled sources are described in the African Craton, the Congo River (Garzanti et al., 2019) or Parana River, South America (Garzanti et al., 2021). An analogue basin developed in similar tectonic conditions where black shales are followed by sandy deposition could

be the Late Ordovician Appalachian Basin (Ettensohn & Lierman, 2015). Another possible analogue is the Magrebian flysch basin situated between Africa and a continental Mediterranean block during the Oligocene–Miocene times (Martín-Martín et al., 2020). Basin floor deposits deflection by bathymetry in narrow basins with active tectonics has been documented in confined turbidite systems (Joseph & Lomas, 2004) such as in the Apennine foredeep basin in Italy (Tinterri & Muzzi Magalhaes, 2011), or Tyee forearc basin in Oregon, USA (Santra et al., 2013). However, sandstone interfingering between distinct basin floor fan systems is less well documented because the facies (deep-water turbidites) would be similar and there are not many systems that have a distinct sediment provenance like Kliwa and Fusaru. In deep lake basins which form basin floor fans such as Miocene of Dacian (Fongngern et al., 2016) and Pannonian (Sztanó et al., 2013), interfingering, multidirectional sediment sourced basin floor fans were inferred from seismic data. In the case of our documented Kliwa and Fusaru interfingering systems, despite the lack of seismic data, further studies can quantify the degree of interfingering preserved in the stratigraphy along the basin and infer the tectonic evolution of source-to-sink sedimentary systems during the Oligocene.

6 | CONCLUSIONS

The new sedimentological, petrographical and palaeontological quantitative data, coupled with the U–Pb chronology of detrital zircons, led to the reconstruction of the main sedimentary routing systems of the Moldavides foreland basin and associated source areas during the late Oligocene to early Miocene time.

Based on the analysis of thick deep-water deposits, two main sedimentary systems feeding sediments to the basin floor from opposite eastern and western margins of the foreland basin were interpreted. A third southern system is inferred to be sourced in the south, also on the foreland side of the convergent margins.

The Moldavides Basin, with Fusaru and Kliwa turbidites, is likely typical for marine foreland basins in an active tectonic setting where source-to-sink sedimentary systems will be asymmetrical with different characteristics from fluvial to deep-water fans on the tectonically active and tectonically 'passive'. The eastern quartz arenite Kliwa turbiditic systems were fed by large and low-gradient rivers from the East European Platform/Craton and possibly its western margin was involved in the Variscan deformations.

The Kliwa-type sediments interfingered on the basin floor with the western lithic arenite Fusaru turbidites system, fed by short steep-gradient rivers, from the basement of the Dacia mega-unit (Bucovinian and Getic nappes), and especially by recycling the Cretaceous deposits of the Ceahlău, Teleajen and Audia nappes, already incorporated in the internal thin skin nappes of East Carpathians.

The eastward migration of the East Carpathian orogenic belt front forced the Fusaru system to overlap the top of the Kliwa system during the late Oligocene–early Miocene time based on calcareous nannoplankton biozones NP25-NN1 (Chattian for Lower Kliwa Formation) and maximum depositional age of detrital zircons (22.2 Ma) and the NN2 biozone (Aquitanian for top Fusaru Formation). The youngest clusters of detrital zircons from the Fusaru Formation (21.32–26.67 Ma) suggest that regional arc volcanism started in the latest Oligocene, slightly older than published age data.

The main control factor affecting source-to-sink sedimentary systems must have been the late Palaeogene–Miocene collision, which affected the geometry of the western active margin of the foreland basin, as well as the back bulge area on the opposite eastern side.

Since these stratigraphical units are continuous along much of the East Carpathian's front, our model and interpretations are likely valid further north in similar Oligo–Miocene deposits in Ukraine and the Polish Carpathian.

ACKNOWLEDGEMENTS

Deep gratitude to Piotr Krzywiec, Tomas N. Capaldi and the anonymous reviewer, whose comments and suggestions have substantially improved the quality of the manuscript. This work was supported by grants from the Romanian Executive Agency for Higher Education, Research, Development and Inovation, UEFISCDI: PN-III-P4-PCE-2021-0901, dir. R.D.R., Project PN-III-P4-PCE-2020-0971 dir. MM-D and PN-III-P4-ID-PCCF-2016-0014 dir. M.M-D.

CONFLICT OF INTEREST

The authors declared no conflict of interest.

PEER REVIEW

The peer review history for this article is available at https://publons.com/publon/10.1111/bre.12711.

DATA AVAILABILITY STATEMENT

The data that support the findings of this study are openly available in The provenance of Oligocene lithic and quartz arenites at https://osf.io/n87a4, reference number DOI: 10.17605/OSF.IO/N87A4.

ORCID

Relu D. Roban https://orcid.org/0000-0003-4423-432X
Ioan Munteanu https://orcid.org/0000-0003-4040-0570
Victor Barbu https://orcid.org/0000-0003-0450-7514

REFERENCES

Allen, P. A. (2017). *Sediment routing systems: The fate of sediment from source to sink* (p. 407). Cambridge University Press. https://doi.org/10.1017/9781316135754

Anastasiu, N., Popa, M., & Vîrban, B. (1994). Oligocene turbiditic sequences of the East Carpathians (Romania): Facies analysis, arhitecture and cyclic events. *Studii și Cercetări. Geologie, Geofizică, Geografie, seria Geologie*, *39*, 35–43.

Andreescu, I., Codrea, V., Lubenescu, V., Munteanu, T., Petculescu, A., Ştiucă, E., & Terzea, E. (2013). New developments in the upper Pliocene–Pleistocene stratigraphic units of the Dacian Basin (Eastern Paratethys), Romania. *Quaternary International*, *284*, 15–29. https://doi.org/10.1016/j.quaint.2012.02.009

Bădescu, D. (2005). *Evoluția tectono-stratigrafică a Carpaților Orientali în decursul Mezozoicului și Neozoicului* (p. 308). Universitatea din București.

Balintoni, I., & Balica, C. (2013). Carpathian peri-Gondwanan terranes in the East Carpathians (Romania): A testimony of an Ordovician, north-African orogeny. *Gondwana Research*, *23*, 1053–1070. https://doi.org/10.1016/j.gr.2012.07.013

Balintoni, I., & Balica, C. (2016). Peri-Amazonian provenance of the Euxinic Craton components in Dobrogea and of the North Dobrogean Orogen components (Romania): A detrital zircon study. *Precambrian Research*, *278*, 34–51. https://doi.org/10.1016/j.precamres.2016.03.008

Balintoni, I., Balica, C., Ducea, M. N., & Hann, H.-P. (2014). Peri-Gondwanan terranes in the Romanian Carpathians: A review of their spatial distribution, origin, provenance, and evolution. *Geoscience Frontiers*, *5*, 395–411. https://doi.org/10.1016/j.gsf.2013.09.002

Balintoni, I., Balica, C., Ducea, M. N., Hann, H. P., & Şabliovschi, V. (2010). The anatomy of a Gondwanan terrane: The Neoproterozoic–Ordovician basement of the pre-Alpine Sebeş–Lotru composite terrane (South Carpathians, Romania). *Gondwana Research*, *17*, 561–572. https://doi.org/10.1016/j.gr.2009.08.003

Balintoni, I., Balica, C., Ducea, M. N., & Stremţan, C. (2011). Peri-Amazonian, Avalonian-type and Ganderian-type terranes in the South Carpathians, Romania: The Danubian domain basement. *Gondwana Research*, *19*, 945–957. https://doi.org/10.1016/j.gr.2010.10.002

Balintoni, I., Balica, C., Seghedi, A., & Ducea, M. N. (2010). Avalonian and Cadomian terranes in North Dobrogea, Romania. *Precambrian Research*, *182*, 217–229. https://doi.org/10.1016/j.precamres.2010.08.010

Balintoni, I., Balica, C., Seghedi, A., & Ducea, M. N. (2011). Peri-Amazonian provenance of the central Dobrogea terrane (Romania) attested by U/Pb detrital zircon age patterns, geologica carpathica. *Geologica Carpathica*, *62*, 299–307. https://doi.org/10.2478/v10096-011-0023-x

Barrier, E., Vrielynck, B., Brouillet, J.-F. & Brunet, M.-F. (2018). *Paleotectonic reconstruction of the central Tethyan Realm*. Tectonono-Sedimentary-Palinspastic Maps from Late Permian to Pliocene. CCGM/CGMW, Atlas of 20 Maps (scale: 1/15 000 000).

Bibikova, E. V., Claesson, S., Fedotova, A. A., Stepanyuk, L. M., Shumlyansky, L. V., Kirnozova, T. I., Fugzan, M. M., & Il'insky, L.S. (2013). Isotope-geochronological (U-Th-Pb, Lu-Hf) study of the zircons from the Archean magmatic and metasedimentary rocks of the Podolia domain, Ukrainian shield. *Geochemistry International*, *51*, 87–108. https://doi.org/10.1134/S0016702913020031

Bibikova, E. V., Fedotova, A. A., Claesson, S., & Stepanyuk, L. M. (2015). Early crust of the Podolia domain of the Ukrainian shield: Isotopic age of terrigenous zircons from quartzites of the bug group. *Stratigraphy and Geological Correlation*, *23*, 555–567. https://doi.org/10.1134/S0869593815060027

Bouma, A. H. (1962). *Sedimentology of some flysch deposits* (p. 168). Elsevier.

Burchfiel, B. C., & Nakov, R. (2015). The multiply deformed foreland fold-thrust belt of the Balkan Orogen, Northern Bulgaria. *Geosphere*, *11*, 463–490. https://doi.org/10.1130/ges01020.1

Carrigan, C. W., Mukasa, S. B., Haydoutov, I., & Kolcheva, K. (2005). Age of Variscan magmatism from the Balkan sector of the orogen, central Bulgaria. *Lithos*, *82*, 125–147. https://doi.org/10.1016/j.lithos.2004.12.010

Contescu, L., Jipa, D., Mihăilescu, N., & Panin, N. (1966). The internal paleogene flysch of the Eastern Carpathians: Paleocurents, source areas and facies significance. *Sedimentology*, *7*, 307–321.

Cvetković, V., Poli, G., Christofides, G., Koroneos, A., Pécskay, Z., Resimić-Šarić, K., & Erić, V. (2007). The miocene granitoid rocks of Mt. Bukulja (central Serbia): Evidence for Pannonian extension-related granitoid magmatism in the Northern Dinarides. *European Journal of Mineralogy*, *19*, 513–532. https://doi.org/10.1127/0935-1221/2007/0019-1736

Decelles, P., & Giles, K. A. (1996). Foreland basin systems. *Basin Research*, *8*, 105–123. https://doi.org/10.1046/j.1365-2117.1996.01491.x

Dicea, O. (1996). Tectonic setting and hydrocarbon habitat of the Romanian external Carpathians. In P. A. Ziegler & F. Horvath (Eds.), *Peri-tethys memoir 2: Structure and prospects of alpine basins and forelands* (Vol. *170*, pp. 403–425). Mémoires Du Museum National D'histoire Naturelle.

Dickinson, W. R. (1985). Interpreting provenance relations from detrital modes of sandstones. In G. G. Zuffa (Ed.), *Provenance of arenites* (pp. 333–361). Springer. https://doi.org/10.1007/978-94-017-2809-6_15

Doglioni, C., Busatta, C., Bolis, G., Marianini, L., & Zanella, M. (1996). Structural evolution of the Eastern Balkans (Bulgaria). *Marine and Petroleum Geology*, *13*, 225–251. https://doi.org/10.1016/0264-8172(95)00045-3

Dott, R. H. (1964). Wacke, graywacke and matrix-what approach to immature sandstone classification? *Journal of Sedimentary Research*, *34*, 625–632. https://doi.org/10.1306/74D71109-2B21-11D7-864800102C1865D

Ducea, M. N., Bârlă, A., Stoica, A. M., Panaiotu, C., & Petrescu, L. (2020). Temporal-geochemical evolution of the Perşani volcanic field, eastern Transylvanian basin (Romania): Implications for Slab Rollback beneath the SE Carpathians. *Tectonics*, *39*, e2019TC005802. https://doi.org/10.1029/2019TC005802

Ducea, M. N., Giosan, L., Carter, A., Balica, C., Stoica, A. M., Roban, R. D., Balintoni, I., Filip, F., & Petrescu, L. (2018). U-Pb detrital zircon geochronology of the lower Danube and its tributaries: Implications for the geology of the Carpathians. *Geochemistry, Geophysics, Geosystems*, *19*, 3208–3223. https://doi.org/10.1029/2018GC007659

Ducea, M. N., Negulescu, E., Profeta, L., Săbău, G., Jianu, D., Petrescu, L., & Hoffman, D. (2016). Evolution of the Sibişel shear zone (south Carpathians): A study of its type locality

near Răşinari (Romania) and tectonic implications. *Tectonics*, *35*, 2131–2157. https://doi.org/10.1002/2016tc004193

Duchesne, J.-C., Laurent, O., Gerdes, A., Bonin, B., Liégeois, J.-P., Tatu, M., & Berza, T. (2017). Source constraints on the genesis of Danubian granites in the South Carpathians alpine belt (Romania). *Lithos*, *294–295*, 198–221. https://doi.org/10.1016/j.lithos.2017.10.002

Duchesne, J.-C., Liègeois, J.-P., Iancu, V., Berza, T., Matukov, D. I., Tatu, M., & Sergeev, S. A. (2008). Post-collisional melting of crustal sources: Constraints from geochronology, petrology and Sr, Nd isotope geochemistry of the Variscan Sichevita and Poniasca Granitoid Plutons (South Carpathians, Romania). *International Journal of Earth Sciences*, *97*, 705–723. https://doi.org/10.1007/s00531-007-0185-z

Dziadzio, P. S., Matyasik, I., Garecka, M., & Szydło, A. (2016). *Lower oligocene menilite beds, polish outer Carpathians: Supposed deep-sea flysch locally reinterpreted as shelfal, based on new sedimentological, micropalaeontological and organic-geochemical data* (p. 120). Instytut Nafty i Gazu - Państwowy Instytut Badawczy. https://doi.org/10.18668/PN2016.213

Ellouz, N., & Roca, E. (1994). Palinspastic reconstructions of the Carpathians and adjacent areas since the Cretaceous: A quantitative approach. In F. Roure (Ed.), *Peri-tethyan platforms* (pp. 51–78). Editions Technip.

Ettensohn, F. R., & Lierman, R. T. (2015). Using black shales to constrain possible tectonic and structural influence on foreland-basin evolution and Cratonic Yoking: Late Taconian Orogeny, late Ordovician Appalachian basin, Eastern USA. *Geological Society, London, Special Publications*, *413*, 119–141. https://doi.org/10.1144/SP413.5

Fongngern, R., Olariu, C., Steel, R. J., & Krézsek, C. (2016). Clinoform growth in a miocene, para-tethyan deep lake basin: Thin topsets, irregular foresets and thick bottomsets. *Basin Research*, *28*, 770–795. https://doi.org/10.1111/bre.12132

Francovschi, I., Grădinaru, E., Li, H., Shumlyanskyy, L., & Ciobotaru, V. (2021). U–Pb geochronology and Hf isotope systematics of detrital zircon from the late Ediacaran Kalyus beds (East European Platform): Palaeogeographic evolution of Southwestern Baltica and constraints on the Ediacaran Biota. *Precambrian Research*, *355*, 106062. https://doi.org/10.1016/j.precamres.2020.106062

Fügenschuh, B., & Schmid, S. M. (2005). Age and significance of core complex formation in a very curved orogen: Evidence from fission track studies in the South Carpathians (Romania). *Tectonophy*, *404*, 33–53. https://doi.org/10.1016/j.tecto.2005.03.019

Gągała, Ł., Vergés, J., Saura, E., Malata, T., Ringenbach, J.-C., Werner, P., & Krzywiec, P. (2012). Architecture and orogenic evolution of the northeastern outer Carpathians from cross-section balancing and forward modeling. *Tectonophysics*, *532–535*, 223–241. https://doi.org/10.1016/j.tecto.2012.02.014

Gallhofer, D., Quadt, A. V., Peytcheva, I., Schmid, S. M., & Heinrich, C. A. (2015). Tectonic, magmatic, and metallogenic evolution of the late Cretaceous arc in the Carpathian-Balkan Orogen. *Tectonics*, *34*, 1813–1836. https://doi.org/10.1002/2015TC003834

Garzanti, E. (2019). Petrographic classification of sand and sandstone. *Earth-Science Reviews*, *192*, 545–563. https://doi.org/10.1016/j.earscirev.2018.12.014

Garzanti, E., Limonta, M., Vezzoli, G., & Sosa, N. (2021). From Patagonia to Río De La Plata: Multistep long-distance littoral transport of Andean Volcaniclastic sand along the argentine passive margin. *Sedimentology*, *68*, 3357–3384. https://doi.org/10.1111/sed.12902

Garzanti, E., Vermeesch, P., Vezzoli, G., Andò, S., Botti, E., Limonta, M., Dinis, P., Hahn, A., Baudet, D., De Grave, J., & Yaya, N. K. (2019). Congo river sand and the equatorial quartz factory. *Earth-Science Reviews*, *197*, 102918. https://doi.org/10.1016/j.earscirev.2019.102918

Gedl, P., & Worobiec, E. (2020). Origin and timing of palaeovalleys in the Carpathian Foredeep basement (Sędziszów Małopolski-Rzeszów area; SE Poland) in the light of palynological studies. *Marine and Petroleum Geology*, *115*, 104277. https://doi.org/10.1016/j.marpetgeo.2020.104277

Gehrels, G. (2014). Detrital zircon U-Pb geochronology applied to tectonics. *Annual Review of Earth and Planetary Sciences*, *42*, 127–149. https://doi.org/10.1146/annurev-earth-050212-124012

Gehrels, G. E., Valencia, V. A., & Ruiz, J. (2008). Enhanced precision, accuracy, efficiency, and spatial resolution of U-Pb ages by laser ablation–multicollector–inductively coupled plasma–mass spectrometry. *Geochemistry, Geophysics, Geosystems*, *9*(3), Q03017. https://doi.org/10.1029/2007GC001805

Gigliuto, L. G., Grasu, C., Loiacono, F., Miclăuş, C., Moretti, E., Puglisi, D., & Raffaelli, G. (2004). Provenance changes and sedimentology of the eocene–oligocene "moldovița lithofacies" of the Tarcău Nappe (Eastern Carpathians, Romania). *Geologica Carpathica*, *66*, 299–309.

Gradstein, F. M., Ogg, J. G., Smith, A. G., Agterberg, F. P., Bleeker, W., Cooper, R. A., Davydov, V., Gibbard, P., Hinnov, L. A., House, M. R., Lourens, L., Luterbacher, H.-P., McArthur, J., Melchin, M. J., Robb, L. J., Shergold, J., Villeneuve, M., Wardlaw, B. R., Ali, J., … Wilson, D. (2004). *A geologic time scale 2004* (p. 589). Cambridge University Press. https://doi.org/10.1017/CBO9780511536045

Grasu, C., Catană, C., & Grindea, D. (1988). *Carpathian flysch. Petrography and economic considerations (in Romanian)* (p. 208). Techical Publishing House.

Hippolyte, J. C., Săndulescu, M., Bădescu, D., & Bădescu, N. (1996). L'activite D'un segment De La Ligne Tornquist-Teissere Depuis Le Jurassique Superieur: La Faille De Peceneaga-Camena (Roumanie). *Comptes rendus de l'Académie des Sciences*, *323*, 1043–1050.

Horváth, F., Musitz, B., Balázs, A., Végh, A., Uhrin, A., Nádor, A., Koroknai, B., Pap, N., Tóth, T., & Wórum, G. (2015). Evolution of the Pannonian basin and its geothermal resources. *Geothermics*, *53*, 328–352. https://doi.org/10.1016/j.geothermics.2014.07.009

Hoskin, P. W. O., & Schaltegger, U. (2003). The composition of zircon and igneous and metamorphic petrogenesis. *Reviews in Mineralogy and Geochemistry*, *53*(1), 27–62. https://doi.org/10.2113/0530027

Jarosiński, M., Poprawa, P., & Ziegler, P. A. (2009). Cenozoic dynamic evolution of the polish platform. *Geological Quarterly*, *53*(1), 3–26. https://gq.pgi.gov.pl/article/view/7502

Jipa, D. (1966). Relationship between longitudinal and transversal currents in the paleogene of the Tarcău Valley (Eastern Carpathians). *Sedimentology*, *7*, 299–305. https://doi.org/10.1111/j.1365-3091.1966.tb01296.x

Jipa, D. C., Panin, N., Olariu, C., & Pop, C. (2020). Black sea submarine valleys—Patterns, systems, networks. *Geo-Eco-Marina*, *26*, 15–40. https://doi.org/10.5281/zenodo.4682752

Joseph, P., & Lomas, S. A. (2004). Deep-water sedimentation in the alpine basin of SE France: New perspectives on the Grès

d'Annot and related systems. *Geological Society, London, Special Publications*, *221*, 448. https://doi.org/10.1144/GSL.SP.2004.221

Jovanović, D., Cvetković, V., Erić, S., Kostić, B., Peytcheva, I., & Šarić, K. (2019). Variscan granitoids of the East Serbian Carpatho-Balkanides: New insight inferred from U–Pb zircon ages and geochemical data. *Swiss Journal of Geosciences*, *112*, 121–142. https://doi.org/10.1007/s00015-018-0325-4

Kounov, A., Gerdjikov, I., Vangelov, D., Balkanska, E., Lazarova, A., Georgiev, S., Blunt, E., & Stockli, D. (2017). First thermochronological constraints on the cenozoic extension along the Balkan fold-thrust belt (Central Stara Planina Mountains, Bulgaria). *International Journal of Earth Sciences (Geol Rundsch)*, *107*(4), 1515–1538. https://doi.org/10.1007/s00531-017-1555-9

Kounov, A., & Schmid, S. M. (2012). Fission-track constraints on the thermal and tectonic evolution of the Apuseni mountains (Romania). *International Journal of Earth Sciences*, *102*, 207–233. https://doi.org/10.1007/s00531-012-0800-5

Kováč, M., Hudáčková, N., Halásová, E., Kováčová, M., Holcová, K., Oszczypko-Clowes, M., Báldi, K., Less, G., Nagymarosy, A., Ruman, A., Klučiar, T., & Jamrich, M. (2017). The central paratethys palaeoceanography: A water circulation model based on microfossil proxies, climate, and changes of depositional environment. *Acta Geologica Slovakia*, *9*(1), 75–114.

Krézsek, C., Bercea, R. I., Tari, G., & Ionescu, G. (2017). Cretaceous sedimentation along the Romanian margin of the Black Sea: Inferences from onshore to offshore correlations. In M. D. Simmons, G. C. Tari, & A. I. Okay (Eds.), *Petroleum geology of the Black Sea* (Vol. *464*, pp. 211–245). Geological Society of London, Special Publication. https://doi.org/10.1144/SP464.10

Krzywiec, P., Gągała, Ł., Mazur, S., Słonka, Ł., Kufrasa, M., Malinowski, M., Pietsch, K., & Golonka, J. (2017). Variscan deformation along the Teisseyre-Tornquist zone in Se Poland: Thick-skinned structural inheritance or thin-skinned thrusting? *Tectonophysics*, *718*, 83–91. https://doi.org/10.1016/j.tecto.2017.06.008

Krzywiec, P., & Stachowska, A. (2016). Late Cretaceous inversion of the NW segment of the Mid-Polish Trough—How marginal troughs were formed, and does it matter at all? *Zeitschrift der Deutschen Gesellschaft für Geowissenschaften Band*, *167*, 107–119. https://doi.org/10.1127/zdgg/2016/0068

Książkiewicz, M. (1975). Bathymetry of the Carpathian flysch basin. *Acta Gelogica Polonica*, *25*, 309–367.

Leever, K. A., Bertotti, G., Zoetemeijer, R., Matenco, L., & Cloetingh, S. (2006). The effects of a lateral variation in lithospheric strength on Foredeep evolution: Implications for the East Carpathian Foredeep. *Tectonophysics*, *421*, 251–267. https://doi.org/10.1016/j.tecto.2006.04.020

Leever, K. A., Matenco, L., Bertotti, G., Cloetingh, S., & Drijkoningen, G. G. (2006). Late orogenic vertical movements in the Carpathian bend zone—Seismic constraints on the transition zone from Orogen to Foredeep. *Basin Research*, *18*, 521–545. https://doi.org/10.1111/j.1365-2117.2006.00306.x

Liégeois, J. P., Berza, T., Tatu, M., & Duchesne, J. C. (1996). The neoproterozoic pan-African basement from the alpine lower Danubian Nappe system (south Carpathians, Romania). *Precambrian Research*, *80*, 281–301. https://doi.org/10.1016/S0301-9268(96)00019-8

Lorentzen, S., Braut, T., Augustsson, C., Nystuen, J. P., Jahren, J., & Schovsbo, N. H. (2020). Provenance of lower Cambrian quartz arenite on southwestern Baltica: Weathering versus recycling. *Journal of Sedimentary Research*, *90*, 493–512. https://doi.org/10.2110/jsr.2020.20

Lowe, D. R. (1982). Sediment gravity flows: II. Depositional models with special reference to the deposits of high-density turbidity currents. *Journal of Sedimentary Research*, *52*, 279–297. https://doi.org/10.1306/212F7F31-2B24-11D7-8648000102C1865D

Martín-Martín, M., Guerrera, F., Miclăuș, C., & Tramontana, M. (2020). Similar Oligo-Miocene tectono-sedimentary evolution of the paratethyan branches represented by the Moldavidian basin and Maghrebian flysch basin. *Sedimentary Geology*, *396*, 105548. https://doi.org/10.1016/j.sedgeo.2019.105548

Matenco, L. (2017). Tectonics and exhumation of Romanian Carpathians: Inferences from kinematic and thermochronological studies. In M. Rădoane & A. Vespremeanu-Stroe (Eds.), *Landform dynamics and evolution in Romania* (pp. 15–56). Springer International Publishing.

Matenco, L., & Bertotti, G. (2000). Tertiary tectonic evolution of the external east Carpathians (Romania). *Tectonophysics*, *316*, 255–286. https://doi.org/10.1016/S0040-1951(99)00261-9

Matenco, L., Krézsek, C., Merten, S., Schmid, S., Cloetingh, S., & Andriessen, P. (2010). Characteristics of collisional orogens with low topographic build-up: An example from the Carpathians. *Terra Nova*, *22*, 155–165. https://doi.org/10.1111/j.1365-3121.2010.00931.x

Matenco, L., & Schmid, S. (1999). Exhumation of the Danubian Nappes System (South Carpathians) during the early tertiary: Inferences from kinematic and paleostress analysis at the getic/Danubian Nappes contact. *Tectonophysics*, *314*, 401–422. https://doi.org/10.1016/S0040-1951(99)00221-8

Mazur, S., Krzywiec, P., Malinowski, M., Lewandowski, M., Aleksandrowski, P., & Mikolajczak, M. (2018). On the nature of the Teisseyre-Tornquist zone. *Geology, Geophysics & Environment*, *44*(1), 17–30. https://doi.org/10.7494/geol.2018.44.1.17

Mazur, S., Mikolajczak, M., Krzywiec, P., Malinowski, M., Lewandowski, M., & Buffenmyer, V. (2016). Pomeranian Caledonides, NW Poland—A collisional suture or thin-skinned fold-and-thrust belt? *Tectonophysics*, *692*, 29–43. https://doi.org/10.1016/j.tecto.2016.06.017

McBride, E. F. (1963). A classification of common sandstones. *Journal of Sedimentary Research*, *33*, 664–669. https://doi.org/10.1306/74D70EE8-2B21-11D7-8648000102C1865D

Medaris, G., Ducea, M., Ghent, E., & Iancu, V. (2003). Conditions and timing of high-pressure variscan metamorphism in the South Carpathians, Romania. *Lithos*, *70*, 141–161. https://doi.org/10.1016/s0024-4937(03)00096-3

Melinte, C. M. (2005). Oligocene palaeoenvironmental changes in the Romanian Carpathians, revealed by calcareous nannofossils. *Studia Geologica Polonica*, *124*, 341–352.

Merten, S., Matenco, L., Foeken, J. P. T., Stuart, F. M., & Andriessen, P. A. M. (2010). From nappe stacking to out-of-sequence postcollisional deformations: Cretaceous to quaternary exhumation history of the Se Carpathians assessed by low-temperature thermochronology. *Tectonics*, *29*, 1–28. https://doi.org/10.1029/2009tc002550

Miall, A. D. (2000). *Principles of sedimentary basin analysis (third, updated and enlarged edition)* (p. 616). Springer-Verlag. https://doi.org/10.1007/978-3-662-03999-1

Miclăuș, C., Loiacono, F., Puglisi, D., & Baciu, S. D. (2009). Eocene-Oligocene sedimentation in the external areas of the Moldavide

basin (marginal folds Nappe, Eastern Carpathians, Romania): Sedimentological, paleontological and petrographic approaches. *Geologica Carpathica*, *60*, 397–417. https://doi.org/10.2478/v10096-009-0029-9

Miller, K. G., Browning, J. V., Schmelz, W. J., Kopp, R. E., Mountain, G. S., & Wright, J. D. (2020). Cenozoic sea-level and cryospheric evolution from deep-sea geochemical and continental margin records. *Science Advances*, *6*, eaaz1346. https://doi.org/10.1126/sciadv.aaz1346

Morely, C. K. (1996). Models for relative motion of crustal blocks within the Carpathian region, based on restorations of the outer Carpathian thrust sheets. *Tectonics*, *15*, 885–904. https://doi.org/10.1029/95TC03681

Mulder, T., & Alexander, J. (2001). The physical character of subaqueous sedimentary density flows and their deposits. *Sedimentology*, *48*, 269–299. https://doi.org/10.1046/j.1365-3091.2001.00360.x

Necea, D., Juez-Larré, J., Mațenco, L., Andriessen, P. A. M., & Dinu, C. (2021). Foreland migration of orogenic exhumation during nappe stacking: Inferences from a high-resolution thermochronological profile over the southeast Carpathians. *Global and Planetary Change*, *200*, 103457. https://doi.org/10.1016/j.gloplacha.2021.103457

Nilsen, T. H., Shew, R. D., Steffens, G. S., & Studlick, J. R. J. (2007). Atlas of deep-water outcrops. *AAPG Studies in Geology*, *56*, 504. https://doi.org/10.1306/St561240

Nyberg, B., Helland-Hansen, W., Gawthorpe, R. L., Sandbakken, P., Eide, C. H., Sømme, T., Hadler-Jacobsen, F., & Leiknes, S. (2018). Revisiting morphological relationships of modern source-to-sink segments as a first-order approach to scale ancient sedimentary systems. *Sedimentary Geology*, *373*, 111–133. https://doi.org/10.1016/j.sedgeo.2018.06.007

Oaie, G., Seghedi, A., Rădan, S., & Vaida, M. (2005). Sedimentology and source area composition for the Neoproterozoic-Eocambrian turbidites from East Moesia. *Geologica Belgica*, *8*(4), 78–98.

Oszczypko, N. (2006). Late Jurassic-Miocene evolution of the Outer Carpathian fold-and-thrust belt and its foredeep basin (Western Carpathians, Poland). *Geological Quarterly*, *50*, 169–194.

Paraschiv, D. (1979). *Platforma Moesică și zăcămintele ei de hidrocarburi* (p. 195). Editura Academiei Republicii Socialiste România.

Peytcheva, I., Tacheva, E., von Quadt, A., & Nedialkov, R. (2018). U-Pb zircon and titanite ages and Sr-Nd-Hf isotope constraints on the timing and evolution of the Petrohan-Mezdreya pluton (Western Balkan Mts, Bulgaria). *Geologica Balcanica*, *47*(2), 25–46. https://doi.org/10.52321/GeolBalc.47.2.25

Popescu, B. (1995). Romania's petroleum systems and their remaining potential. *Petroleum Geoscience*, *1*, 337–350. https://doi.org/10.1144/petgeo.1.4.337

Popov, S. V., Rögl, F., Rozanov, A. V., Steininger, F., Shcherba, I. G., & Kovac, M. (Eds.). (2004). *Lithological-paleogeographic maps of paratethys 10 maps late eocene to pliocene* (p. 46). Schweizerbart Science Publishers.

Posamentier, H. W., & Walker, R. G. (2006). Deep water turbidites and turbiditic fans. In H. W. Posamentier & R. G. Walker (Eds.), *Facies models revisited* (pp. 399–527). Society for Sedimentary Geology. https://doi.org/10.2110/pec.06.84

Răbagia, T., Roban, R. D., & Tărăpoancă, M. (2011). Sedimentary records of paleogene (eocene to lowermost miocene) deformations near the contact between the Carpathian thrust belt and Moesia. *Oil & Gas Science and Technology–Revue d'IFP Energies Nouvelles*, *66*, 931–952. https://doi.org/10.2516/ogst/2011146

Roban, R. D., Ducea, M. N., Mațenco, L., Panaiotu, G. C., Profeta, L., Krézsek, C., Melinte-Dobrinescu, M. C., Anastasiu, N., Dimofte, D., Apotrosoaei, V., & Francovschi, I. (2020). Lower Cretaceous provenance and sedimentary deposition in the Eastern Carpathians: Inferences for the evolution of the subducted oceanic domain and its European passive continental margin. *Tectonics*, *39*, e2019TC005780. https://doi.org/10.1029/2019TC005780

Roban, R.D., Ducea, M.N., Mihalcea, V., Luffi, P., Ioan Munteanu I., Victor Barbu, V., Tiliță M., Vlăsceanu M., & Ene V. (2022) *Constraining the onset of subduction through sediment provenance changes: the Ceahlău-Severin Ocean of the Eastern Carpathians*, 11th International Symposium on the Cretaceous System, Warsaw (Poland) Abstract Volume (pp. 316-317). Gimpo-Print Bartlomiej Pohl.

Roban, R. D., Krézsek, C., & Melinte-Dobrinescu, M. C. (2017). Cretaceous sedimentation in the outer Eastern Carpathians: Implications for the facies model reconstruction of the Moldavide basin. *Sedimentary Geology*, *354*, 24–42. https://doi.org/10.1016/j.sedgeo.2017.04.001

Rögl, F. (1999). Mediterranean and paratethys. Facts and hypotheses of an oligocene to miocene paleogeography. *Geologica Carpathica*, *50*, 339–349.

Roure, F., Roca, E., & Sassi, W. (1993). The neogene evolution of the outer Carpathian flysch units (Poland, Ukraine and Romania): Kinematics of a foreland/fold-and-thrust belt system. *Sedimentary Geology*, *86*, 177–201. https://doi.org/10.1016/0037-0738(93)90139-v

Rusu, A. (1988). Oligocene events in Transylvania (Romania) and the first separation of Paratethys. *Dări de Seamă ale Insitutului de Geologie și Geofizică*, *72–73*, 207–223.

Sachsenhofer, R. F., Hentschke, J., Bechtel, A., Coric, S., Gratzer, R., Gross, D., Horsfield, B., Rachetti, A., & Soliman, A. (2015). Hydrocarbon potential and depositional environments of Oligo-Miocene rocks in the Eastern Carpathians (Vrancea Nappe, Romania). *Marine and Petroleum Geology*, *68*, 269–290. https://doi.org/10.1016/j.marpetgeo.2015.08.034

Sachsenhofer, R. F., Popov, S. V., Bechtel, A., Coric, S., Francu, J., Gratzer, R., Grunert, P., Kotarba, M., Mayer, J., Pupp, M., Rupprecht, B. J., & Vincent, S. J. (2018). Oligocene and lower Miocene source rocks in the Paratethys: Palaeogeographical and stratigraphic controls. In M. D. Simmons, G. C. Tari, & A. I. Okay (Eds.), *Petroleum geology of the black sea* (Vol. *464*, pp. 267–306). Geological Society of London, Special Publication. https://doi.org/10.1144/SP464.1

Saintot, A., Brunet, M.-F., Yakovlev, F., Sebrier, M., Stephenson, R., Ershov, A., Chalot-Prat, F., & Mccann, T. (2006). The Mesozoic-Cenozoic tectonic evolution of the greater Caucasus. *Geological Society, London, Memoirs*, *32*, 277–289. https://doi.org/10.1144/GSL.MEM.2006.032.01.16

Salata, D., & Uchman, A. (2019). Provenance of upper oligocene to lower Miocene Krosno formation sandstones in the Skole Nappe (Southeast Poland): New insights from heavy minerals. *Geological Journal*, *55*, 4625–4641. https://doi.org/10.1002/gj.3695

Sanders, C., Andriessen, P., & Cloetingh, S. (1999). Life cycle of the East Carpathian Orogen: Erosion history of a doubly vergent critical wedge assessed by fission track thermochronology. *Journal of Geophysical Research*, *104*, 29095–29112.

Săndulescu, M. (1984). *Geotectonica României [Geotectonics of Romania]* (p. 343). Editura Tehnică.

Săndulescu, M. (1988). Cenozoic tectonic history of the Carpathians. In L. H. Royden & F. Horvath (Eds.), *The Pannonian basin, a study in Basin evolution* (Vol. *45*, pp. 17–25). AAPG Memoir.

Săndulescu, M., Kräutner, H. G., Balintoni, I., Russo-Săndulescu, D., & Micu, M. (1981). The structure of the East Carpathians (Moldavia-Maramures area). *Guide Exc. B1, XII Congress of the Carpathian Balkan Geological Association*, *B1*, 92.

Săndulescu, M., Ştefănescu, M., Butac, A., Pătruţ, I., & Zaharescu, P. (1981). Genetical and structural relations between Flysch and Molasse (the East Carpathians). *Guide Exc. B1, XII Congress of the Carpathian Balkan Geological Association*, *A5*, 95.

Santra, M., Steel, R. J., Olariu, C., & Sweet, M. L. (2013). Stages of sedimentary prism development on a convergent margin—Eocene Tyee Forearc Basin, Coast Range, Oregon, USA. *Global and Planetary Change*, *103*, 207–231. https://doi.org/10.1016/j.gloplacha.2012.11.006

Saulea, E., Popescu, I., & Săndulescu, J. (Eds.). (1969). *Atlasul litofacial, 1:200,000 (in Romanian and French)*. IGR.

Schieber, J., Miclăuş, C., Seserman, A., Liu, B., & Teng, J. (2019). When a mudstone was actually a "sand": Results of a sedimentological investigation of the bituminous marl formation (oligocene), Eastern Carpathians of Romania. *Sedimentary Geology*, *384*, 12–28. https://doi.org/10.1016/j.sedgeo.2019.02.009

Schmid, S., Bernoulli, D., Fügenschuh, B., Maţenco, L., Schefer, S., Schuster, R., Tischler, M., & Ustaszewski, K. (2008). The alpine-Carpathian-Dinaridic orogenic system: Correlation and evolution of tectonic units. *Swiss Journal of Geosciences*, *101*, 139–183. https://doi.org/10.1007/s00015-008-1247-3

Schmid, S. M., Fügenschuh, B., Kounov, A., Maţenco, L., Nievergelt, P., Oberhänsli, R., Pleuger, J., Schefer, S., Schuster, R., Tomljenović, B., Ustaszewski, K., & Van Hinsbergen, D. J. J. (2020). Tectonic units of the alpine collision zone between Eastern Alps and Western Turkey. *Gondwana Research*, *78*, 308–374. https://doi.org/10.1016/j.gr.2019.07.005

Seghedi, A. (2001). The north Dobrogea Orogenic belt (Romania); A review. In P. A. Ziegler, W. Cavazza, A. F. Robertson, & S. Crasquin-Soleau (Eds.), *Peri-Tethys Memoir 6; Peri-Tethyan Rift/Wrench Basins and Passive Margins* (Vol. *186*, pp. 237–257). Memoires Du Museum National D'histoire Naturelle.

Seghedi, A., Berza, T., Iancu, V., Mărunţiu, M., & Oaie, G. (2005). Neoproterozoic terranes in the Moesian basement and in the alpine Danubian Nappes of the South Carpathians. *Geologica Belgica*, *8*(4), 4–19.

Seghedi, I., Maţenco, L., Downes, H., Mason, P. R. D., Szakács, A. & Pécskay, Z. (2011). Tectonic significance of changes in post-subduction pliocene–quaternary magmatism in the south east part of the Carpathian–Pannonian region. *Tectonophysics*, *502*, 146–157. https://doi.org/10.1016/j.tecto.2009.12.003

Shumlyanskyy, L., Billström, K., Hawkesworth, C., & Elming, S.-Å. (2012). U-Pb age and Hf isotope compositions of zircons from the north-western region of the Ukrainian shield: Mantle melting in response to post-collision extension. *Terra Nova*, *24*, 373–379. https://doi.org/10.1111/j.1365-3121.2012.01075.x

Shumlyanskyy, L., Hawkesworth, C., Dhuime, B., Billström, K., Claesson, S., & Storey, C. (2015). 207pb/206pb ages and Hf isotope composition of zircons from sedimentary rocks of the Ukrainian shield: Crustal growth of the south-western part of east European Craton from Archaean to Neoproterozoic. *Precambrian Research*, *260*, 39–54. https://doi.org/10.1016/j.precamres.2015.01.007

Sømme, T. O., Helland-Hansen, W., Martinsen, O. J., & Thurmond, J. B. (2009). Relationships between morphological and sedimentological parameters in source-to-sink systems: A basis for predicting semi-quantitative characteristics in subsurface systems. *Basin Research*, *21*, 361–387. https://doi.org/10.1111/j.1365-2117.2009.00397.x

Ştefănescu, M. (1976). O nouă imagine a structurii flişului intern din regiunea de curbură a Carpaţilor. *Dari de Seamă ale Insitutului de Geologie şi Geofizică*, *LXII*, 257–259.

Ştefănescu, M., Dicea, O., Butac, A., & Ciulavu, D. (2006). Hydrocarbon geology of the Romanian Carpathians, their foreland and the Transylvanian basin. In J. Golonka & F. J. Picha (Eds.), *The Carpathians and their foreland: Geology and hydrocarbon resources* (Vol. *84*, pp. 521–567). AAPG Memoir. https://doi.org/10.1306/985619M843077

Ştefănescu, M., Gheţa, N., & Dicea, M. (1979). On the Oligo-Miocene boundary in the external flysh zone of the Carpathian bend (between the Teleajen Valley and the Dâmboviţa Valley). A tentative solving by Calcareous Nannoplankton. *Revue Roumaine de Géologie, Géophysique et Géographie: Série de Géologie*, *23*, 89–94.

Ştefănescu, M., Popescu, I., Melinte, M., Ivan, V., Ştefănescu, M., Papaianopol, I., Popescu, G., & Dumitrică, P. (2018). *Harta Geologică a României, Scara 1: 50 000, Foaia 112d, L-35-89-D*. Nehoiu.

Ştefănescu, M., Popescu, I., Ştefănescu, M., Ivan, V., Melinte, M. C., & Stănescu, V. (1993). Aspects of the possibilities of lithological correlation of the oligocene—Lower miocene deposits of the Buzău Valley. *Romanian Journal of Stratigraphy*, *75*, 83–91.

Stern, R. J. (1994). Arc assembly and continental collision in the neoproterozoic east African orogen: Implications for the consolidation of Gondwanaland. *Annual Review of Earth and Planetary Sciences*, *22*(1), 319–351. https://doi.org/10.1146/annurev.ea.22.050194.001535

Stoica, A. M., Ducea, M. N., Roban, R. D., & Jianu, D. (2016). Origin and evolution of the South Carpathians basement (Romania): A zircon and monazite geochronologic study of its alpine sedimentary cover. *International Geology Review*, *58*, 510–524. https://doi.org/10.1080/00206814.2015.1092097

Suttner, L. J., Basu, A., & Mack, G. H. (1981). Climate and the origin of quartz arenites. *Journal of Sedimentary Research*, *51*, 1235–1246. https://doi.org/10.1306/212F7E73-2B24-11D7-8648000102C1865D

Sylvester, Z., & Lowe, D. R. (2004). Textural trends in turbidites and slurry beds from the oligocene flysch of the East Carpathians, Romania. *Sedimentology*, *51*, 945–972. https://doi.org/10.1111/j.1365-3091.2004.00653.x

Sztanó, O., Szafián, P., Magyar, I., Horányi, A., Bada, G., Hughes, D. W., Hoyer, D. L., & Wallis, R. J. (2013). Aggradation and progradation controlled clinothems and deep-water sand delivery model in the Neogene Lake Pannon, Makó Trough, Pannonian Basin, SE Hungary. *Global and Planetary Change*, *103*, 149–167. https://doi.org/10.1016/j.gloplacha.2012.05.026

Tărăpoancă, M., Bertotti, G., Maţenco, L., Dinu, C., & Cloetingh, S. (2003). Architecture of the Focşani depression: A 13 km deep basin in the Carpathians bend zone (Romania). *Tectonics*, *22*(6), 1074. https://doi.org/10.1029/2002TC001486

Tărăpoancă, M., Garcia-Castellanos, D., Bertotti, G., Maţenco, L., Cloetingh, S. A. P. L., & Dinu, C. (2004). Role of the 3-D distributions of load and lithospheric strength in orogenic arcs:

Polystage subsidence in the Carpathians Foredeep. *Earth and Planetary Science Letters*, *221*, 163–180. https://doi.org/10.1016/S0012-821X(04)00068-8

Tichomirowa, M., Käßner, A., Sperner, B., Lapp, M., Leonhardt, D., Linnemann, U., Münker, C., Ovtcharova, M., Pfänder, J. A., Schaltegger, U., Sergeev, S., Von Quadt, A., & Whitehouse, M. (2019). Dating multiply overprinted granites: The effect of protracted magmatism and fluid flow on dating systems (Zircon U-Pb: Shrimp/sims, La-Icp-Ms, Ca-Id-Tims; and Rb–Sr, Ar–Ar)—Granites from the Western Erzgebirge (Bohemian Massif, Germany). *Chemical Geology*, *519*, 11–38. https://doi.org/10.1016/j.chemgeo.2019.04.024

Tiliță, M., Lenkey, L., Maţenco, L., Horváth, F., Surányi, G., & Cloetingh, S. (2018). Heat flow modelling in the Transylvanian basin: Implications for the evolution of the intra-Carpathians area. *Global and Planetary Change*, *171*, 148–166. https://doi.org/10.1016/j.gloplacha.2018.07.007

Tinterri, R., & Muzzi Magalhaes, P. (2011). Synsedimentary structural control on foredeep turbidites: An example from Miocene Marnoso-Arenacea formation, Northern Apennines, Italy. *Marine and Petroleum Geology*, *28*, 629–657. https://doi.org/10.1016/j.marpetgeo.2010.07.007

Van Hinsbergen, D. J. J., Torsvik, T. H., Schmid, S. M., Maţenco, L. C., Maffione, M., Vissers, R. L. M., Gürer, D., & Spakman, W. (2020). Orogenic architecture of the mediterranean region and kinematic reconstruction of its tectonic evolution since the Triassic. *Gondwana Research*, *81*, 79–229. https://doi.org/10.1016/j.gr.2019.07.009

Vangelov, D., Gerdjikov, Y., Kounov, A., & Lazarova, A. (2013). The Balkan fold-thrust belt: An overview of the main features. *Geologica Balcanica*, *42*, 29–47.

Vermeesch, P. (2021). Maximum depositional age estimation revisited. *Geoscience Frontiers*, *12*, 843–850. https://doi.org/10.1016/j.gsf.2020.08.008

Vinogradov, C., Pârvu, C., Bomboe, P., & Negoiţă, V. (1983). *Petrologia Aplicată a Rocilor Detritice* (p. 264). Editura Academiei Republicii Socialiste România.

Vlăsceanu, M., Ducea, M. N., Luffi, P., Bârlă, A., & Seghedi, I. (2021). Carpathian-Pannonian magmatism database. *Geochemistry, Geophysics, Geosystems*, *22*, e2021GC009970. https://doi.org/10.1029/2021GC009970

Von Raumer, J. F., Bussy, F., Schaltegger, U., Schulz, B., & Stampfli, G. M. (2013). Pre-mesozoic alpine basements—Their place in the European Paleozoic framework. *GSA Bulletin*, *125*, 89–108. https://doi.org/10.1130/B30654.1

Żelaźniewicz, A., Buła, Z., Fanning, M., Seghedi, A., & Żaba, J. (2009). More evidence on Neoproterozoic terranes in southern Poland and southeastern Romania. *Geological Quarterly*, *53*, 93–124.

Żelaźniewicz, A., Oberc-Dziedzic, T., & Slama, J. (2020). Baltica and the Cadomian Orogen in the Ediacaran–Cambrian: A perspective from Se Poland. *International Journal of Earth Sciences*, *109*, 1503–1528. https://doi.org/10.1007/s00531-020-01858-0

SUPPORTING INFORMATION

Additional supporting information can be found online in the Supporting Information section at the end of this article.

How to cite this article: Roban, R. D., Ducea, M. N., Mihalcea, V. I., Munteanu, I., Barbu, V., Melinte-Dobrinescu, M. C., Olariu, C., & Vlăsceanu, M. (2022). Provenance of Oligocene lithic and quartz arenites of the East Carpathians: Understanding sediment routing systems on compressional basin margins. *Basin Research*, *00*, 1–27. https://doi.org/10.1111/bre.12711